Review

Homogeneous and Heterogeneous Catalysis of Glucose to Lactic Acid and Lactates: A Review

Thomas Saulnier-Bellemare and Gregory S. Patience*

Read Online

ACCESS | Metrics & More | Article Recommendations

ABSTRACT: The current societal demand to replace polymers derived from petroleum with sustainable bioplastics such as polylactic acid (PLA) has motivated industry to commercialize ever-larger facilities for biobased monomers like lactic acid. Even though most of the lactic acid is produced by fermentation, long reaction times and high capital costs compromise the economics and thus limit the appeal of biotechnological processes. Catalytic conversion of hexose from biomass is a burgeoning alternative to fermentation. Here we identify catalysts to convert glucose to lactic acid, along with their proposed mechanisms. High Lewis acidity makes erbium salts among the most active homogeneous catalysts, while solvent coordination with the metal species polarize the substrate, increasing the catalytic activity. For heterogeneous catalysts, Sn-containing bimetallic systems combine the high Lewis acidity of Sn while moderating it with another metal, thus decreasing byproducts. Hierarchical bimetallic Sn-Beta zeolites combine a high number of open sites catalyzing glucose isomerization in the mesoporous regions and the confinement effect assisting fructose retro-aldol in microporous regions, yielding up to 67% lactic acid from glucose. Loss of activity is still an issue for heterogeneous catalysts, mostly due to solvent adsorption on the active sites, coke formation, and metal leaching, which impedes its large scale adoption.
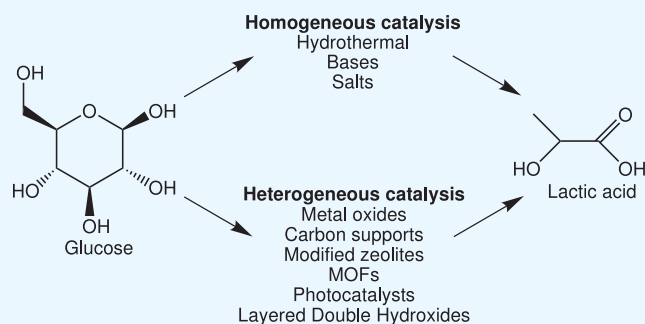
INTRODUCTION

To reduce societies' dependence on fossil resources, alternative carbon sources must be adopted. Biomass is the most abundant carbon source in nature, making it a promising low-cost feedstock for the chemical industry. The global biobased plastics market is expected to quadruple by 2030, reaching 43 billion USD,[1] of which polylactic acid (PLA) is a compelling alternative for packaging due to its favorable mechanical and optical properties.[2]

Biotechnological process plants have been built with capacities up to 140 kta to produce lactic acid (LA), a monomer that condenses directly to PLA and a feedstock for lactide (also for PLA) from biomass.[3] However, the high cost and long reaction times of enzymes engender prohibitive investment and operating costs that reach $1,200/t of LA, dragging down operating margins.[3] Chemocatalytic processes potentially improve margins with lower investment costs due to shorter reaction times and the ability to operate over a wider range of reaction conditions. Biomass monosaccharides such as glucose rapidly degrade under hydrothermal conditions to multiple products, of which LA is produced in small yields.[4,5] A large range of homogeneous and heterogeneous catalysts have been tested to convert glucose to LA over the last 20 years. Among them, rare metal salts have been identified as the most efficient homogeneous catalysts due to their high Lewis

acidities, achieving LA yields over 85%.[6−8] Such a performance has yet to be achieved in heteregeneous catalytic systems due to leaching of the rare metal species.[9,10] Other metal salt combinations that tune the Lewis acidity improve LA yield. Hierarchical bimetallic Sn-Beta zeolite is the most promising heterogeneous catalyst due to its pore system and Lewis acidity leading to LA yields over 65%.[11−14] Other bifunctionalized aluminosilicates attain LA yields over 60% due to their well-tuned Lewis acidities accelerating the rate-determining retro-aldol decomposition of fructose. Reusability is still an issue with Lewis acidic aluminosilicates primarily due to solvent adsorption on the active sites, decreasing accessibility. Coke formation and metal leaching are other important causes of deactivation. More advanced catalysts, such as photocatalysts and layered double hydroxides, reach LA yields over 70%, but their technological development stage is much lower than that of other catalysts.[15−18] More research to build a catalyst that is
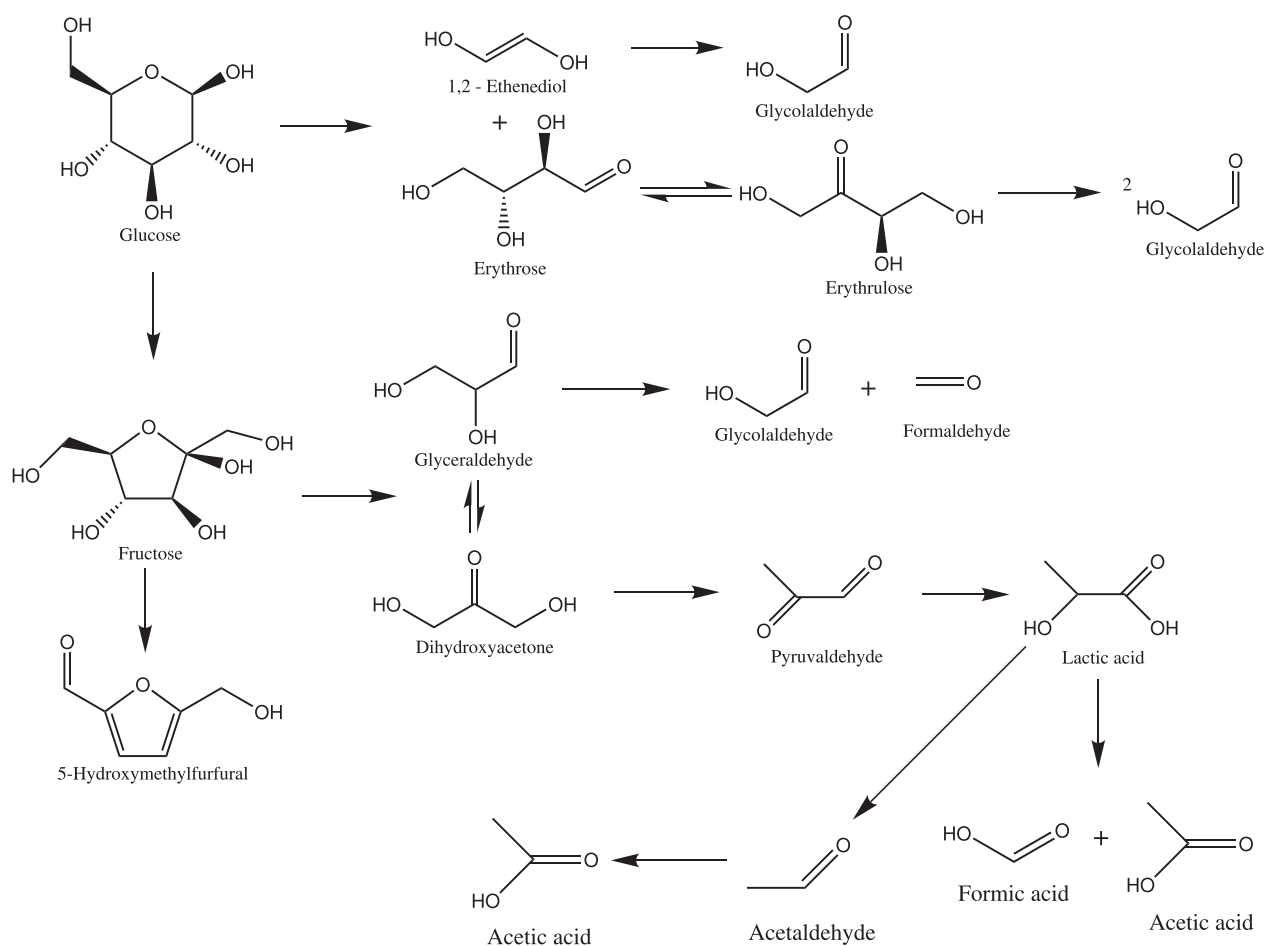
Figure 1. Proposed glucose reaction mechanism to LA.

both highly efficient and stable is required to develop a profitable biobased lactic acid process. This review article aims to highlight the characteristics of the most promising catalysts and identify the key research pathways to investigate.

■ HOMOGENEOUS CATALYSIS

Hydrothermal Conditions. Water in hydrothermal conditions undergoes autoprotolysis, generating Brønsted basicity and acidity able to catalyze sugar reactions.[19] The dissociation constant, K_W, depends on the difference of chemical potential between pure water and its ions, controlled both by density and by the internal energy of the medium.

Glucose undergoes retro-aldol decomposition when exposed to ionized water in hydrothermal conditions. This concerted reaction is a base-assisted proton transfer from C3−OH to C1═O, cleaving the C2−C3 bond and producing both erythrose (4C) and 1,2-ethenediol (2C)[20] (Figure 1). 1,2-Ethenediol rapidly isomerizes to glycolaldehyde.[21] Erythrose reacts to its erythrulose isomer, which is more thermodynamically stable. In supercritical conditions, erythrulose may undergo a second retro-aldol reaction, yielding two glyco-laldehyde molecules[22] (Figure 1). In subcritical conditions, most of the erythrulose is formed in equilibrium with erythrose in the presence of some glycolaldehyde. Moreover, glyco-laldehyde might react to LA in a base-catalyzed mechanism, yielding 28% LA at 300 °C, 0.75 M NaOH, and 10 min. As the C3 intermediates are reactive species, the low LA yields are

due to the prevalence of secondary reactions, notably forming methanol, formic acid, or dimers by aldol condensation.[4]

Glucose isomerizes at high temperature to fructose in the presence of Brønsted bases following the Lobry de Bruyn−van Ekenstein transformation.[23] Matsuoka et al. (2012) observed that fructose yields start to rise in hydrothermal conditions starting at 220 °C, while most of the glucose reacts forming glycolaldehyde. At 250 °C, fructose yield peaks after 20 min to decrease afterward due to retro-aldol or dehydration reactions.[20] Cantero et al. (2015) achieved 20% LA yield, along with 15% glyceraldehyde within 5 s in a continuous reactor operating at 300 °C and 10 MPa.[5] Sasaki et al. (2002) observed that the isomerization product yields peak at 400 °C and 25 MPa due to the lower K_W at higher temperature caused by the transition from subcritical to supercritical conditions. Meanwhile, low temperatures enhance dehydration product yields such as 5-(hydroxymethyl)furfural (5-HMF) and 1,6-anhydro-D-glucose.[22] This highlights the fact that dehydration products are thermodynamic products, while retro-aldol product yields, such as LA, are controlled kinetically. Moreover, dehydration reactions are catalyzed by strong Brønsted acidity, less present in hydrothermal conditions.

Kinetic studies have demonstrated that, in subcritical water, glyceraldehyde decomposes to glycolaldehyde and form-aldehyde by a water ion-assisted reaction. In supercritical water, radical decomposition of glyceraldehyde is the domninant reaction pathway, resulting in the formation of glycolaldehyde, formaldehyde, formic acid, and acetaldehyde.
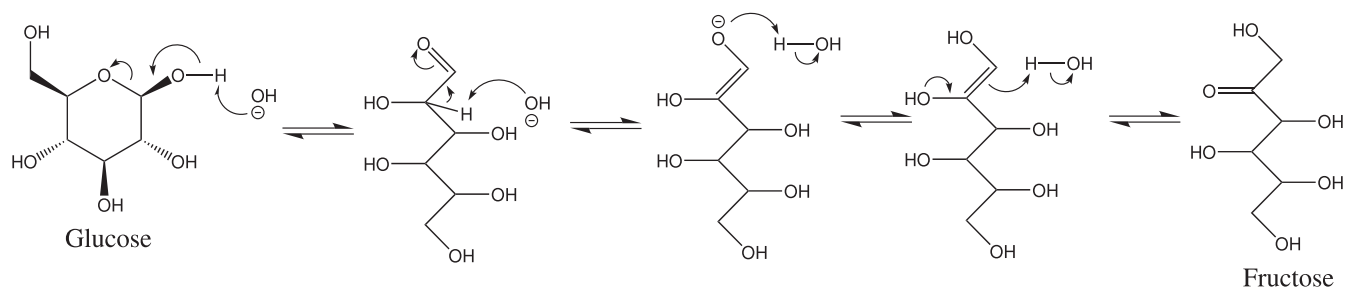
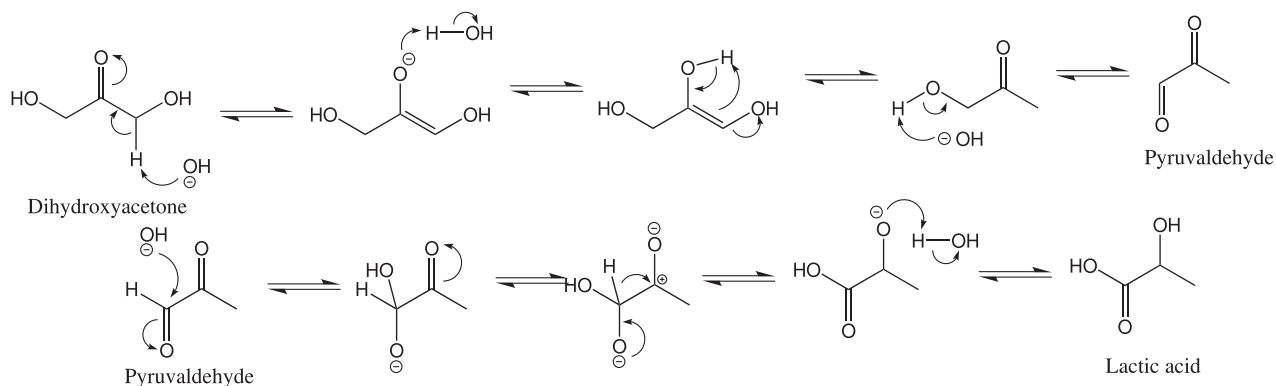**Figure 2.** Base-catalyzed glucose isomerization mechanism.

Figure 3. Cannizzaro-type reaction mechanism from DHA to LA.

Long reaction times favor gasification to CO_2 in subcritical conditions and to CO and H_2 in supercritical conditions.[24] Various other compounds also form at 500 °C due to pyrolysis.[25] Thus, to form LA, it is best to maintain subcritical conditions as it avoids radical-driven reactions leading to undesired products.

Glucose reacts in hydrothermal conditions to fructose, but fructose retro-aldol product yields (glyceraldehyde, dihydroxyacetone (DHA), pyruvaldehyde (PA)) are higher, implying that fructose is highly reactive when exposed to Brønsted basicity. Cantero et al. (2015) measured a 67% PA yield from fructose at 330 °C, at a conversion of 90%.[26] Reaction time influences the composition of the retro-aldol product mixture, as glyceraldehyde slowly isomerizes to DHA and DHA dehydrates to PA. The conversion of PA to LA is a Cannizzaro-type benzilic acid rearrangement followed by a facile dehydration reaction. Benzilic acid rearrangement is catalyzed by both acid and base sites.[27] Water autoprotolysis generating both hydroxyl and hydronium ions, the lactic acid formation rate thus depends solely on K_W.

At 450 °C and <80 MPa, LA dehydrates to acrylic acid as the pressure increases. The acrylic acid then decarboxylates to acetaldehyde, CO_2, and H_2 or decarbonylizes to acetaldehyde, CO, and H_2O. Acetaldehyde partially oxidizes to acetic acid. At higher pressure, the intramolecular dehydration reaction pathway is preferred at a ratio k_{hp}/k_{lp} = 0.76, producing mostly acrylic and propionic acids. Nevertheless, the LA conversion remained below 35% at 450 °C at maximum reaction time for all pressures, showing that LA is a relatively stable compound under hydrothermal conditions.[28]

Water in hydrothermal conditions is thus able to promote various glucose reactions due to autoprotolysis, but it fails to achieve a high LA yield due to the prevalence of secondary reactions, such as glucose retro-aldol degradation, fructose dehydration, and LA decomposition.

Soluble Bases. Soluble bases as homogeneous catalysts produce Brønsted basicity assisting LA production from sugar for all reaction steps. Indeed, glucose isomerization to fructose is catalyzed by Brønsted base sites, as fructose undergoes a base-assisted proton transfer from C2 to C1 after ring opening (Figure 2). OH^- ions are also involved for fructose retro-aldol to C3 intermediates and subsequent Cannizzaro-type reactions to form LA (Figure 3).

To produce the Brønsted base sites needed for glucose catalysis to LA, the solid bases have to dissociate. Hence, reaction yields are heavily influenced by the solubility of the bases. Accordingly, Shen et al. (2009) transformed glycerin in 1.25 M KOH, NaOH, or LiOH, yielding respectively 90, 87, and 81% LA at 300 °C for 90 min. Solubilities for these bases are 122 g L^{-1} for KOH, 109 g L^{-1} for NaOH, and 13 g L^{-1} for LiOH at 294 K, matching the same sequence for solubility as for LA yields.[29] Ma et al. (2010) reported the same trend, producing 45% LA from fructose at 300 °C for 60 s with KOH and 40% LA from NaOH at the same conditions (Table 1).[30] A similar trend has been noted by Yan et al. (2008), who reported LA yields of 14% using 0.8 M KOH on glucose in hydrothermal conditions for 660 s and 12% LA yield in 0.8 M NaOH.[31] Sánchez et al. (2014), however, found no significant difference between 0.5 M KOH and 0.5 M NaOH assisting bread residue transformation to LA at 300 °C in 30 min, both yielding 37(2)% LA.[32] This could be due to polysaccharide hydrolysis to monosaccharides undermining solubility effects, as polysaccharides' slow degradation is promoted by Brønsted acidity arising from water autoprotolysis.

With alkaline earth bases, the larger cations are able to conjugate with two oxygens in a bidentate mode. This coordination mode was first mentioned by Okuyama et al. (1982), who reported a kinetic effect from the addition of divalent ionic salts for hydride shifts in Cannizzaro-type reactions, such as the DHA-to-LA reaction steps. This is due to

Table 1. Soluble Base Catalytic Performances

reactant	catalyst	conditions	conversion	LA yield	ref
cellulose	1.75 M NaOH	200 °C, 60 min	N/A	17	36
glucose	2.5 M NaOH	300 °C, 1 min	N/A	27	31
glucose	2.5 M NaOH	300 °C, 1.5 min	N/A	43	30
glycerin	1.25 M KOH	300 °C, 90 min	100	90	29
corncobs	0.7 M Ca(OH)$_2$	300 °C, 30 min	N/A	45	40
DHA	1.1 M Ca(OH)$_2$	25 °C, 300 min	100	59	38
glucose	0.1 M Ba(OH)$_2$	250 °C, 3 min	N/A	57	34
glucose	0.15 M Ba(OH)$_2$, 0.5 M Ca(OH)$_2$	60 °C, 12 h	100	43	41

the stabilization of the transition state (TS) during the hydride shift by chelation.[33] Esposito et al. (2013) identified the role of divalent cations by assessing the LA yields from glucose at 220 °C during 12 h with NaOH (17% LA yield), Ba(OH)$_2$ (53% LA yield), and a combination of NaOH/BaCl$_2$ (40% LA yield).[34] This yield enhancement with the presence of divalent cations is attributable to the coordination of Ba^{2+} to the two double-bonded oxygens in PA, stabilizing the TS during the hydride shift reaction to LA. Such a yield enhancement was also observed for Ca(OH)$_2$ (49% LA) and Sr(OH)$_2$ (40% LA), implying that an analogous mechanism is encountered for other alkaline earth bases.[34] Li et al. (2017) found a similar effect by switching from monovalent to divalent cations at room temperature during 48 h in a nitrogen atmosphere with DHA, achieving 87% LA yield in Ba(OH)$_2$ at optimal conditions.[35] They also highlighted the importance of the alkaline earth base solubility, as no catalytic effect was observed over the insoluble Mg(OH)$_2$. When O$_2$ was introduced in the reactor's atmosphere, the LA yield dropped quickly and byproducts such as malonic acid, formic acid, and CO$_2$ appeared.[35] Yan and Qi (2014) described the formation of malonic and formic acids from cellulose hydrothermal degradation in the presence of 2.5 M NaOH, identifying that DHA hydrates to malonic acid, while glyceraldehyde decarboxylates to formic acid and CO$_2$.[36]

DHA dimerizes by aldol condensation at high base concentration and high temperature (Figure 4). These dimers either react back to DHA or polymerize to form humins.[37−39]
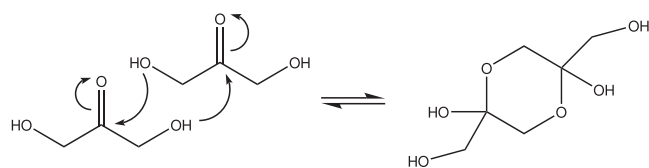
Figure 4. DHA dimerization by aldol condensation mechanism.

After 1 h at room temperature, Ba(OH)$_2$ reached 30% LA for Ca(OH)$_2$ from DHA, which follows the solubilities of both bases.[38,42] However, after 6 h, the LA yield with Ca(OH)$_2$ increases to 58% LA while Ba(OH)$_2$ produces only 50% LA (Table 1).[38] This is likely due to barium complexation with lactates in a monodentate mode, inducing a C1−C2 bond cleavage by polarizing the substrate. Indeed, the degradation

product concentrations pattern match those associated with lactic acid degradation.[29] The nucleophilic attack of OH$^-$ on the lactate complex completes the LA decomposition to formic and acetic acids (Figure 5).[29,41] Cations with larger ionic radii complex more with lactate and thus cause more product degradation by stabilizing the TSs to the undesired products. Moreover, Ca^{2+} degrades less LA than Ba^{2+} due to the lower alkalinity and lower solubility of Ca(OH)$_2$. Combining Ca(OH)$_2$ and Ba(OH)$_2$ respectively at 0.5 and 0.15 M yielded a maximal LA yield at 43% from glucose at 60 °C in 12 h in nitrogen (Table 1).[41] In that dual-catalyst system, Ba(OH)$_2$ provides alkalinity and divalent cations to promote the glucose-to-LA reaction. In the meantime, the total alkalinity is controlled by Ca(OH)$_2$ dissociation and replenishment, inducing a controlled-release catalytic system. Furthermore, Ca^{2+} has a stronger binding ability with lactate than Ba^{2+} and calcium lactate is more stable than LA, inhibiting LA degradation.[41]

The most complete study on the mechanism of alkaline earth bases on glucose to LA was published by Zhao et al. (2022), who used diffusion ordered spectroscopy nuclear magnetic resonance (DOSY NMR) and isotopic labels to identify the coordination states.[43] In basic conditions, Ba^{2+} complexes with water, giving [Ba(OH)(H$_2$O)$_2$]$^+$. The presence of OH$^-$ groups in the solution coupled with the weak acidity of glucose enables pyranose coordination with [Ba(OH)(H$_2$O)$_2$]$^+$, opening the ring and facilitating the isomerization to fructose through a C2−C1 hydride shift. Subsequent retro-aldol with aqueous Ba(OH)$_2$ happens instantly after glucose isomerization to generate glyceraldehyde and DHA. DHA, assisted by barium complexation, dehydrates to PA, releasing the Ba complex. The two double-bonded oxygens on PA may then coordinate again with the Ba complex to get barium lactate through rehydration and benzilic acid rearrangement.[43]

Hence, Ba(OH)$_2$ is the most effective soluble base for glucose catalysis to LA with a maximum observed LA yield from glucose in water of 57% (Table 1).[34] To counter Ba-assisted LA degradation, Ca(OH)$_2$ can be used in combination with Ba(OH)$_2$, thus increasing LA yields. However, the use of soluble bases comes with safety issues and high cost due to the high alkalinity of the system and the low reusability of the catalysts,[44] decreasing their attractiveness for industry.

Salts. Homogeneous catalysis has been tested not only with bases but also with salts, highlighting the activities of the different metal cations. The type of metal species has an effect on the coordination mode, while the LA yield is affected not only by the Lewis acid character of the cation but also by its hydration capability, its oxidation state, and the anion composing the salt.

Lewis acidity is the parameter having the most effect on LA yields when salts are used.[45] Bicker et al. (2005) first tested several metal sulfates on sucrose and DHA, finding that the LA yield follows the sequence of the Lewis acidity of the tested salts, with ZnSO$_4$ being the most efficient catalyst with a LA yield of 39%, compared to NiSO$_4$ and CoSO$_4$, respectively achieving 36 and 31% LA yields (Table 2).[45] Their kinetic study shows that the glucose isomerization reaction has the highest activation energy (102 kJ mol^{-1}), while fructose retro-aldol has a slightly lower activation energy (96 kJ mol^{-1}), and the PA transformation to LA activation energy is much lower (58 kJ mol^{-1}) for the ZnSO$_4$-catalyzed reaction.[45] Zn^{2+} polarizes the products in a bidentate coordination mode,
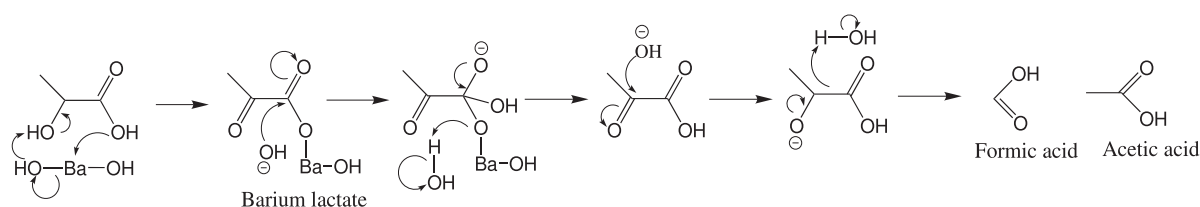
Figure 5. Barium complexation followed by lactate degradation to acetic and formic acid.

Table 2. Salt Catalytic Performances

reactant	catalyst	conditions	conversion	LA yield	ref
DHA	0.005 M AlCl$_3$	140 °C, 90 min	100	98	46
glucose	0.005 M AlCl$_3$, 0.005 M SnCl$_2$	180 °C, 3 MPa, 120 min, pH 2.8	100	81	47
glucose	0.045 M SnCl$_4$, 0.045 M Ba(OH)$_2$	160 °C, 150 min	100	48 ML	50
glucose	0.004 M ZnCl$_2$	200 °C, 180 min, 3% water, 97% CH$_3$OH	N/A	51 ML	9
glucose	400 ppm ZnSO$_4$	300 °C, 3 MPa	N/A	42	45
cellulose	0.007 M Pb(NO$_3$)$_2$	190 °C, 3 MPa, 240 min	100	62	49
cellulose	0.0066 M YCl$_3$	220 °C, 2 MPa, 30 min	100	57	53
rice straw	0.0066 M YCl$_3$	240 °C, 2 MPa, 90 min	N/A	66	52
cellulose	0.012 M ErCl$_3$	240 °C, 2 MPa, 30 min	100	91	7
glucose	0.14% mol La(OTf)$_3$	250 °C, 60 min	N/A	74	56
treated hardwood chips	0.0017 M Er(OTf)$_3$	250 °C, 60 min	N/A	72	58
cellulose	0.0027 M Er(OTf)$_3$	240 °C, 2 MPa, 30 min	100	89.6	6

promoting the Cannizzaro-type reaction to LA. Rasrendra et al. (2010) proposed a similar way of action of the metal cation for Al^{3+} and Cr^{2+}.[46] As proposed by Wang et al. (2017), Zn(II) cations coordinate with two fructose molecules, polarizing the electron cloud of C3 or C4, inducing the C3−C4 bond cleavage to produce both DHA and glyceraldeyde.[9] Deng et al. (2018) came to a high 81% LA yield from glucose by combining Sn(II) and Al(III), with the former exhibiting strong Lewis acidity and the latter showing moderate Lewis acidity (Table 2).[47] In this system, Al(III) catalyzes glucose isomerization and DHA transformation to LA better than Sn(II), due to its binding with a solvent molecule in addition to the bidentate coordination to the substrate, which decreases the Gibbs free energy of activation for glucose isomerization to fructose from 88 to 54 kJ mol^{-1}, based on DFT calculations.[47] Sn(II) catalyzes the retro-aldol reaction, due to its large ionic radius and its closed shell configuration giving it the ability to specifically increase fructose C4−OH group acidity. Its strong Lewis acidity arises primarily from its empty d-orbitals readily interacting with s^2 lone pairs. Sn(II) has a similar electronic configuration as Pb(II), which also efficiently catalyzes glucose to LA (Table 2).[48,49] The estimated ΔG values by density functional theory (DFT) for glucose isomerization are positive for Pb^{2+} but negative for Pb(II)−OH, identifying the promoting effect of solvent coordination on the reaction mechanism. The calculated ΔG is highest for the fructose retro-aldol step, confirming it as the rate-determining reaction step when Lewis acidic salts are used.[49] This solvent promoting effect arises from the added substrate polarization induced by the presence of a vicinal −OH group. Catalyst−solvent interaction was also noted by Zhou et al. (2014), who tested the SnCl$_4$ catalysis of glucose in methanol. In this system, methanol deprotonates due to interaction with SnCl$_4$, which generates Brønsted acidity, thus decreasing the LA yield. Adding NaOH at a molar ratio of 1:1 with the Sn salt to neutralize Brønsted acidity resulted in a methyl lactate (ML) yield increase from 28 to 47%, while dehydration product (5-

HMF, methyl levulinate) yields were cut by more than half (Table 2).[50]

Lanthanide salts interact with water to induce autohydrolysis, resulting in the generation of octahedral complexes.[51−53] Xu et al. (2020) found that these complexes bond more rapidly to the substrate than H$_3$O$^+$, undermining the Brønsted acidity effect.[51] They also found that these complexes assist the specific C$_3$−C$_4$ cleavage during fructose retro-aldol, as it was calculated that the C$_2$−C$_3$ and C$_4$−C$_5$ bond lengths decrease by 0.009−0.019 Å when fructose complexes with Y(III), while the C$_3$−C$_4$ bond length increases by 0.012 Å during the complexation.[51] Such complexes have also been observed with Zr oxide, creating hydrogen bonds with carbohydrates (Figure 6), stabilizing the TS of the Lewis acid catalyzed reactions.[54]
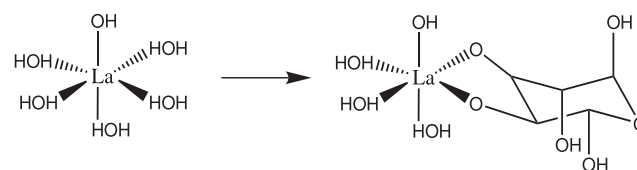

Figure 6. Bidentate coordination of lanthanide octahedral complex with glucose.

LA yields as high as 91% from cellulose and 97% from glucose were observed with ErCl$_3$, which are the highest yields observed to our knowledge (Table 2).[7,55]

Lanthanide triflates have very high Lewis acidities and solubilities and achieve LA yields from glucose in water exceeding 70% (Table 2). LA yield over La(OTf)$_3$ reaches 74% at 180 °C (Table 2). However, when the temperature was raised, humin formation was more prominent due to the autoprotolysis of water in hydrothermal conditions resulting in an increase of Brønsted acidity, decreasing yields.[56] H$_3$O$^+$ in the medium, arising from water autoprotolysis, accelerates the hydrolysis of polysaccharides, increasing the overall LA yields from those molecules. LA yields from cellulose are inversely

proportional to the lanthanide ionic radius, due to an increase in binding ability between the lanthanide and the glucose hydroxyl groups as the radius gets smaller.[6,57] Hence, $Er(OTf)_3$ is the most active catalyst, as erbium possesses the smallest ionic radius of all lanthanides.[6,58] The triflate groups on the lanthanide are stable in water, and the catalyst is reusable, which has not been found with other rare metal salts, where interaction with solvent predomines. In an attempt to make these catalysts heterogeneous, Kim et al. (2020) impregnated $La(OTf)_3$ on SiO_2, but metal leaching and coke were detected, leading to poor reusability.[10]

As for transition metal salts, oxidation state is a determining parameter for catalytic activity. Although a significant product distribution difference was observed between $SnCl_2$ (33% LA yield) and $SnCl_4$ (24% LA yield), it is unclear how the degree of oxidation of Sn affects the reaction mechanism.[59] This is probably due to the $SnCl_2$ species displaying higher Lewis acidity than $SnCl_4$. $SnCl_4$, in turn, would interact more with the solvent, generating more Brønsted acidity, favoring a fructose dehydration mechanism. More work has to be pursued to decipher the mechanistic differences between Sn(II) and Sn(IV) catalyses.

The anion effect on the reaction performance remains controversial. Hayashi et al. (2005) observed a high anion effect on Sn(II) activity, as the ML yield from DHA decreased between $SnCl_2$ (89% ML yield), $SnBr_2$ (83% ML yield), and SnI_2 (71% ML yield), while no ML formation was observed with $SnSO_4$.[60] On the other hand, Rasrendra et al. (2010) tested both chlorine and sulfate salts for a variety of metals without finding a correlation between the anion identity and the catalytic activity.[46] However, Wang et al. (2017) noted a high anion effect on ZnX_2, correlating salt solubility with its catalytic activity. Solubility was insufficient to explain the fact that no EL is formed when $ZnSO_4$ was used, while EL yields up to 30% were observed at 200 °C at 3 h $Zn(NO_3)_2$, 48% with $ZnBr_2$, and 52% with $ZnCl_2$.[9] Zhang et al. (2021) also correlated catalytic performance with solubility for Yb(III) salts.[61] Interestingly, placing $Yb_2(SO_4)_3$ in water decreased the pH of the medium to 3.0. This generation of Brønsted acidity using sulfate could explain the decrease in LA yields, as Brønsted acidity favors fructose dehydration instead of the retro-aldol reaction pathway.[61] Elliot et al. (2018) reported that the catalytic performances of salts of strong acids increase with the salt concentration until it reaches a plateau.[62] Indeed, a low concentration of strong salt is sufficient to get to total conversion, while higher salt concentrations do not affect the reaction. With salts of weak acids, ML yield increases rapidly to form a peak and then decreases slowly with the concentration of salt. This is explained by the fact that, at a certain concentration, Brønsted acidity starts to be generated by the interaction between the cation and the solvent, which favors other products than LA to be formed.[62] However, this does not fully explain the anion effect within the strong acid salt category identified by Hayashi et al. (2005) or the much different performance from an anion to another observed by Rasrendra et al. (2010).[46,60] Hence, an anion effect has been identified by most of the studies on the subject, but the exact way of action of the anion is still to be fully elucidated.

HETEROGENEOUS CATALYSIS

Metal Oxides. Metal oxides present the advantage of being heterogeneous catalysts that are easy to synthesize and study in a large set of conditions. Metal oxides as catalysts are in the form of metallic crystalline frameworks. A few mechanisms have been proposed to explain their catalytic activity. A first mechanism proposes the hydrogenation of the surface oxygens of the framework by the dissociation of water molecules, generating free OH^- ions acting as Brønsted bases (Figure 7).[63,64] The whole reaction mechanism is then the same as for soluble bases.
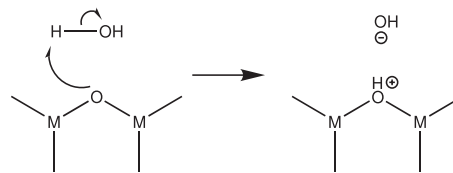

Figure 7. Surface oxide hydrogenation generating Brønsted basicity.

Udomcharoensab et al. (2019) grafted Cu, Co, Ni, and Zn oxides on MgO to generate surface hydroxylated oxygen groups and unsaturated cations, forming Brønsted basic and Lewis acid surface sites.[65] Lewis acidity may also arise from surface oxygens forming M=O groups during calcination.[66,67] When the available surface area decreases, either by structural modifications or particle agglomeration, catalytic activity decreases too, supporting the proposition that the active sites are on the surface of the framework (Figure 8).[68,69]

The activity of both the Lewis acidic metal and the basic surface oxygen were identified on numerous metal oxides, notably by FTIR and CO_2 temperature programmed desorption (TPD).[44,70,71] These vicinal active sites readily coordinate with the substrates, forming two partial bonds with two substrate oxygenated groups. This conjugation polarizes the substrates, promoting the different reaction steps from glucose to LA.[72−74]

The hydroxyl and carbonyl groups in the reaction intermediates (glucose, fructose, PA) coordinate with the surface active sites, promoting every step of the mechanism, except DHA dehydration to PA. This fast reaction step is promoted by the Brønsted acidity arising from water autoprotolysis at high temperature.[71] As for the retro-aldol step, fructose conversion is closely related to Lewis acidity, when comparing the activities of the lowly acidic SnO_2 (83% conversion) and the highly acidic MoO_3 (93% conversion). SnO_2 impregnated with MoO_3 formed a nanostructured dual catalyst, increasing the number of open Sn sites, thus increasing the Lewis acid site density.[75] Other oxides with higher Lewis acidities (Y_2O_3, ZnO, Al_2O_3, TiO_2, ZrO_2) exhibited higher conversions.[76] However, a too high density of Lewis acid sites, as found in Al_2O_3, promoted secondary reactions, decreasing the LA yield. By grafting In on Al_2O_3, Xiao et al. (2021) increased the ML yield until reaching an optimum at 0.12 g g^{-1} (Table 3), as In's weak Lewis acidity moderates Al_2O_3's strong Lewis acid sites.[69] Similarly, by grafting Cr(III) on Al_2O_3 by incipient wetness impregnation, Kosri et al. (2021) achieved 74% LA from glucose, confirming the promoting effect of well-tuned bimetallic Lewis acidic metal systems on glucose reactions.[77]

Hata et al. (2021) tested glucose conversion to LA using TiO_2, Al_2O_3, Nb_2O_5, MgO, ZnO, and Y_2O_3, confirming that both intrinsic Lewis acidity and Brønsted basicity have a considerable effect on the product distribution.[80] XRD detected $Y(OH)_3$ groups at the surface of Y_2O_3 and 0.30 g g^{-1} Y_2O_3/SiO_2 frameworks, which are Brønsted bases and
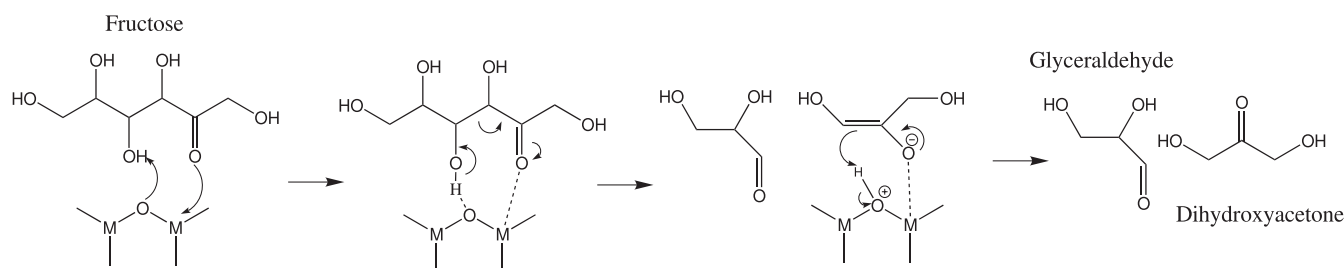
Figure 8. Lewis acid/Brønsted base metal oxide catalyzed fructose retro-aldol to glyceraldehyde and DHA.

Table 3. Metal Oxide Catalytic Performances

reactant	catalyst	conditions	conversion	LA yield	ref
glucose	ZnO	200 °C, 120 min	N/A	42	71
xylose	ZnO	180 °C, 3 MPa, 30 min	92	43	76
glucose	ZnCTAB/MgO	140 °C, 0.4 MPa, 60 min	100	12	65
cellulose	ZrO_2	200 °C, 360 min	87	21	72
DHA	ZrO_2-TiO_2	130 °C, 120 min	100	33 EL	74
glucose	Al_2O_3	160 °C, 0.5 MPa, 360 min	N/A	34 ML	68
glucose	In/Al_2O_3, 0.01 g/L K_2CO_3, 7% water, 93% methanol	180 °C, 2 MPa, 600 min	N/A	49 ML	69
DHA	Sn/Al_2O_3	100 °C, 420 min	95	68	78
fructose	SnO_2/Al_2O_3, 0.3 g/L K_2CO_3	160 °C, 180 min, 98% ethanol	100	61 EL	79
DHA	SnO_2/Nb_2O_5	160 °C, 280 min	100	12	67
glucose	Y_2O_3	200 °C, 1 MPa, 30 min	100	30	80
glucose	Cr/Al_2O_3	170 °C, 1.5 MPa N_2, 360 min	100	74	77

assist the retro-aldol reaction and dehydration of DHA to PA. Y^{3+} arising from the oxide dissociation promotes glucose isomerization to fructose as a Lewis acid in a bidentate coordination mode.[80] A catalytic activity enhancement has been noted by Li et al. (2016) when grafting Y_2O_3 on SiO_2. When grafted, Y_2O_3 is more subject to dissociation, forming the highly Lewis acidic surface Y^{3+}, increasing the cellulose-to-LA yield from 33 to 45%. All the cellulose reacts above 220 °C and 3 h.[81] As for other rare metal heterogeneous catalysts, deactivation by metal leaching is an issue due to their high affinity with water.

Grafting SnO_2 on Al_2O_3 increases the acidity of the catalytic system, increasing the ethyl lactate (EL) yield from DHA from 5 to 70%.[78] Indeed, surface Sn forms open Sn–OH sites, which effectively catalyze this reaction. The effect of open Sn sites has been extensively studied with tin-impregnated zeolite frameworks. Incorporating SnO_2 on a Nb_2O_5 framework also greatly improves the LA yields for both oxides, due to the formation of oxygen vacancies in the framework, increasing Lewis acidity (Table 3).[67] However, Sn has a high concentration of Lewis acid sites, which leads to high lactate yields but also to the formation of more dehydration products.[82] Coupling SnO_2 with ZnO on an Al_2O_3 support instead of Nb_2O_5 addresses this problem by decreasing the Lewis acid site density, avoiding a high 5-HMF yield while keeping a high lactate yield.[79] Hence, the main parameters driving the catalytic reaction are the surface Lewis acid site density and strength.

Apart from catalysis arising from Lewis acidity or basicity, some oxides are involved in the reaction as oxidizing agents in redox reactions. The reduction of the metal species promotes the usual reactions leading to LA production, but they happen at higher temperature and in less time than the usual chemocatalytic reactions. The high temperature slowly degrades LA, yielding a small part of formic acid, while LA is also degraded by electrochemical pathways to acetic acid after 60 s at 300 °C with CuO, the oxide displaying the most electrochemical activity.[83,84] The first step of the electrochemical reaction is the dissociation of the metal oxide to generate cations, which requires alkaline conditions. Indeed, Younas et al. obtained a 9.6% LA yield from rice straws with NiO in water.[85] However, when they added 1 M NaOH, a synergistic effect increased the yield to a high 59% LA, probably due to the base-catalyzed reduction of the oxidized species in the alkaline medium, generating electrochemical activity. They also measured a higher yield using Ni^{2+} over NiO. These results show that the most active sites arise from the dissociation of the metal species generating oxidizing agents, and not from the oxides themselves. The presence of Ni species detected by X-ray diffraction (XRD) after the reaction highlights the electrochemical activity reducing Ni^{2+}.[85] The use of surfactants also enhances redox activity by helping the reduction of the metal species, as it stabilizes the TS during the reaction in the aqueous phase.[86] After transforming glucose to LA with CuO in an alkaline medium, Choudhary et al. (2015) noted the presence of Cu_2O as well as Cu_4O_3, which clearly shows that a redox reaction happens, modifying the oxidation state of Cu(II).[87] Although it is known that CuO participates in redox reactions transforming glucose in LA, the full reaction mechanism is yet to be elucidated.[88]

The use of metal oxides is useful to rapidly test a large variety of metal catalytic performances and identify the mechanism, but the generally low LA yields decrease their chances of being used on an industrial scale.

Carbon Supports. To find a biobased and efficient catalyst support, carbon structures such as graphite, graphite oxide, and graphene oxide are used as catalyst supports. Yu et al. (2019) grafted Al on these three different carbon supports using an air heating method, finding that Al interacts with the oxygen groups of the carbon structure to form active amorphous

Table 4. Carbon-Supported-Catalyst Performances

reactant	catalyst	conditions	conversion	LA yield	ref
glucose	SnO$_2$/AC	160 °C, 360 min	99	45 EL	93
glucose	ZnO/AC	160 °C, 360 min	99	37 EL	94
glucose	Sn−Al/AC	180 °C, 3 MPa, 120 min	100	40	94
glucose	Pb(OH)$_2$/reduced graphene oxide	170 °C, 2.5 MPa, 120 min	100	40	92

octahedral metallic groups. These groups act as Lewis acid sites, assisting glucose isomerization through adsorption/ activation mechanisms. In that way, a maximum 35% fructose yield from glucose using Al−graphene oxide was achieved by microwave heating at 160 °C.[89] However, the catalytic activity of Al−graphene oxide is insufficient to promote fructose retro-aldol at high rates. Graphite is an ineffective support, as its oxygen content is too low to graft a sufficient amount of Al and generate the active sites.[90] Similar conclusions were drawn by Xiong et al. (2020), as they tested Al grafting on graphite oxide and graphene oxide, yielding a 35% fructose yield from glucose for both oxides.[91] On the other hand, a 29% fructose yield was achieved using Al−biochar. This difference in yield is explained not by the difference in Al content but by the Al distribution in the framework. Indeed, graphite and graphene oxides are both more porous than biochar, facilitating the mass transfer to the active sites. The lack of porosity in biochar is partly due to residual lignin and cellulose.[91] Optimization of biochar is yet an interesting path to be investigated, as it is a low-cost, green catalyst support.

Pb^{2+} grafted on graphene oxide nanosheets yielded 59% LA from fructose and 40% from glucose at 160 °C and 2.5 MPa N$_2$ (Table 4).[92] The electrostatic forces of O groups in the graphene oxide framework attract Pb^{2+}, forming Pb(OH)$_2$ detected by XRD, thus providing the Brønsted basicity necessary for fructose retro-aldol and other subsequent reactions to produce LA.[92]

Steam and acid treatments generate carbonyl and hydroxyl groups at the surface of activated carbon (AC), producing weak Brønsted acid sites accelerating the reaction. Al and Sn grafted on activated carbon yield 42% LA from glucose in 20 min at 180 °C (Table 4).[93] A ratio of 1/1 Al/Sn content achieves the best yield, which is consistent with the findings of Deng et al. (2018).[47] Grafting metal oxides on the treated activated carbon also shows high LA yields. SnO$_2$ on AC yields 99% EL from DHA due to its strong acidity arising from open Sn sites. Indeed, acid−base titration showed an increase in acid site concentration between parent AC (0.84 mmol g^{-1}) and SnO$_2$AC (1.37 mmol g^{-1}). From glucose, this strong acidity increases byproduct formation, resulting in a 42% LA yield. ZnO on AC, displaying a lower acid site concentration (0.73 mmol g^{-1}), achieves a lower glucose conversion but a higher selectivity, leading to similar yields as with SnO$_2$ on the carbon support (Table 4).[94] Hence, carbon supports do not offer, for now, LA yields high enough to attract interest in scaling up the process, and more studies have to be done to enhance the catalytic activities of these supports.

N-Heterocyclic carbenes (NHCs), however, display extraordinary activity when used to self-support iridium complexes. Indeed, used in the presence of a soluble base, these catalysts offer almost quantitative LA yields from sorbitol[95] and 93% yield from glycerol.[96] NHCs are strong σ-electron donors, which increases the electron density around the iridium complex.[97] They also enhance the steric bulkiness of the complex, while avoiding clustering of iridium.[95] Thus, this catalyst is more active than homogeneous iridium-based catalysts. Wu et al. (2020) also found that adding ethylene glycol and methanol to the mixture inhibits 2−4 retro-aldol reactions in favor of the 3−3 retro-aldol reaction leading to the formation of lactic acid, due to a displacement of the chemical equilibrium.[95] The presence of a soluble base activates the catalyst by replacing the −CO group on the iridium species by an hydroxyl group. This hydroxyl group initiates the reaction by facilitating a hydrogen transfer from the substrate to the iridium complex, initiating the rate-determining reaction step, either for glycerol dehydration to DHA[98] or for 3−3 retro-aldol for sorbitol.[95] Although it has not been tested until now, it is probable that this NHC−Ir catalyst would also be active for fructose retro-aldol to DHA and glyceraldehyde, which further improves lactic acid selectivity.

Zeolites. Zeolites are the most studied heterogeneous catalysts for glucose reactions to LA due to their high intrinsic acidities and their channel sizes allowing good diffusion. These aluminosilicates are also relatively easy to functionalize. They come in various topologies exhibiting different pore sizes and structures, while being low-cost and generally showing good stability, making them promising catalytic supports.

Functionalization is typically done postsynthesis, requiring dealumination or desilication in order to generate vacant sites, leaving space for other species to be included in the framework. Dealumination is done in harsh acidic conditions where Al sites, which are weak Brønsted and strong Lewis acid sites, are withdrawn from the zeolitic framework. As Al is the minority species in zeolites, with Si/Al ratios being rarely under 15, the crystalline structure is usually preserved. Vacant sites left after dealumination form silanol nests, which are then filled with metals through incipient wetness impregnation, solid state ion exchange, or other postsynthesis methods (Figure 9). Metals grafted by incipient wetness impregnation
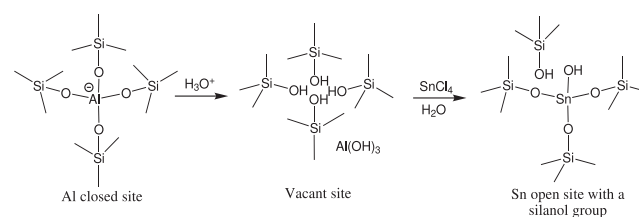

Figure 9. Zeolite postsynthesis functionalization procedure.

only reach the surface vacant sites of the framework, and extraframework metal species are formed.[99] These extraframework metallic species are metal oxide species, cluttering the pores and being generally less active than the same metal grafted on the zeolites. Similarly, solid state ion exchange, which is achieved by grinding solid metal precursors with the dealuminated zeolite, also forms extraframework metal groups. Chemical vapor deposition is able to reach a higher metal fraction in the framework but still generates extraframework metal species, which undermines the LA yields.[100,101] A
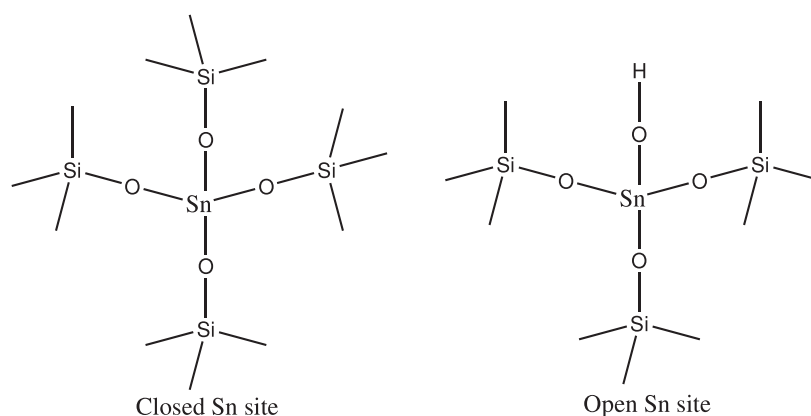
Figure 10. Closed and open site conformations in Sn zeolites.

combination of Ga and Zn was notably grafted on nanozeolites Y by Verma et al. (2017) by incipient wetness impregnation to get the high Lewis acidity of Ga, while neutralizing its Brønsted acidity with the intrinsic basicity of Zn. They got a high 58% ML yield from cellulose along with good reusability.[102]

Apart from dealumination, desilication in highly alkaline medium is another method to generate vacant sites in the zeolitic framework. Mesoporosity emerging from the withdrawal of Si groups forms open Al sites, increasing the Lewis acidity. Dapsens et al. (2013) desilicated Al-MFI with NaOH and structure directing agents to replace silica by aluminum. They achieved 90% LA yield from DHA in 6 h. However, Lewis acid site concentration decreased over the runs, caused by Al leaching.[103] This was also observed by Graça et al. (2018), who desilicated on Na−Al-Beta zeolites to graft Mg in the framework. While Mg leaching was also detected by Yang et al. (2020), who grafted Mg after dealumination, this leaching was more important with desilication.[104,105] This might be due to the weakening of the framework caused by the withdrawal of Si−O links.

Hydrothermal zeolite synthesis is also a method used to functionalize the zeolitic framework. It consists of using raw SiO_2, metal salts and a structure directing agent to synthesize zeolites containing the desired metal. It results in more closed metal sites and less metal leaching.[106,107] However, this method generally necessitates a fluoride medium, which introduces environmental and safety issues to the procedure. Hydrothermal synthesis also requires long crystallization times, from a couple of days to several weeks to get a high degree of crystallinity.[108] Moreover, the atomic radius of the metal included in the framework is usually higher than that of Al, which creates deformities and defects in the framework, limiting its degree of crystallinity and stability. Hence, even though hydrothermal synthesized zeolites are stable and have a high number of closed sites, they possess some drawbacks that hinder their attractiveness for industrial catalysis.

The metals included in the framework occupy two types of site: closed sites and open sites. Closed sites are fully included in the framework, while open sites possess one hydrolyzed M−OH bond, generally vicinal to a silanol group (Figure 10). In Sn-Beta, the most studied catalyst for glucose to LA, closed Sn sites coordinate with glucose in a bidentate way,[109] while open Sn sites, which are more Lewis acidic, coordinate in a monodentate way, as the substrate also coordinates with a vicinal silanol group.[110] DFT calculations demonstrated that the monodentate coordination open site mechanism for

glucose isomerization was energetically favorable compared to the closed site mechanism, as the activation energy when a vicinal silanol group is participating in the transition state is 20 kJ mol^{-1} lower than when it is not participating.[111] Steric interactions between the substrate and the framework are the major reason why monodentate coordination is preferred to bidentate.[112] However, few studies opt for a bidentate coordination mechanism between the open Sn site and the substrate molecule, with the difference of activity between closed and open sites mostly owing to the required geometric distortion for an optimal host−guest interaction being less energetically costly for open sites.[113−115]

The hydrogen atom on the −OH group of the open sites can be replaced by other cations, tuning the catalytic properties of the zeolite. Bermejo-Deval et al. (2014) exchanged H$^+$ with Na$^+$ by adding NaNO$_3$ in the hydrothermal synthesis gel and found that this cation enhances glucose epimerization to mannose via a 1,2 intramolecular carbon shift instead of isomerization to fructose via a 1,2 intramolecular hydride shift due to Na$^+$ strong electrostatic presence stabilizing the epimerization TS.[113,116] Aho et al. (2023) included cations in a Sn−Al-Beta framework to find that Sr/Sn−Al-Beta catalysts produce 53% ML from glucose, highlighting the promoting effect of some Lewis acidic cations on the catalytic activity.[117] On the other hand, surface H$^+$ species add Brønsted acidity to the catalyst, causing more secondary reactions to occur.[118] Exchanging the surface −OH group for a fluoride atom during hydrothermal synthesis makes the pores less hydrophilic, decreasing the solvent adsorption on the active sites, thus making the catalyst more stable.[109] Even though solvent internal diffusion is inhibited in hydrophobic pores, glucose diffuses through the pores by van der Waals attractive interactions.[119]

The presence of a vicinal silanol group inhibits the retro-aldol of fructose. Indeed, silanol groups increase isomerization rates but decrease retro-aldol product yield.[120] Josephson et al. (2018) came to a similar conclusion by studying a Sn-SPP catalyst containing a high density of silanol nests, versus a Sn-Beta catalyst comprising a smaller number of Si−OH groups. They found that fructose in ethanol readily reacts to ethyl fructoside when a silanol group is vicinal to an open Sn center by an S$_N$1 mechanism.[121] Silanol groups also increase the hydrophilicity of the framework, which leads to water adsorption on the active sites. This eventually leads to a decrease in LA yields, as the active sites are less accessible to glucose. LA yield slightly increases over the runs after

Table 5. Various Zeolite Catalytic Performances

reactant	catalyst	conditions	conversion	LA yield	ref
glucose	mesoporous Sn-MCM-41	160 °C, 1200 min	100	43 ML	125
glucose	Zr-SBA-15	240 °C, 2.75 MPa, 360 min	100	48	127
glucose	Sn-Beta	160 °C, 1200 min	99	43 ML	92
glucose	Sn-Beta	200 °C, 4 MPa, 1200 min, 20% GVL	100	72	128
glucose	Sn-Beta	200 °C, 300 min	N/A	68	129
glucose	Sn-Beta, WO_3	160 °C, 0.5 MPa, 300 min	N/A	52	120
glucose	Sn-Beta, $CaSO_4$	200 °C, 300 min	N/A	68	130
glucose	Sn-Beta, SiO_2, SiC	180 °C, 4 MPa, 30 min	100	68	131
glucose	Mg−Sn-Beta	120 °C, 0.4 MPa, 360 min	99	50	120
glucose	In−Sn-Beta	190 °C, 120 min	100	53	132
glucose	Zn−Sn-Beta	190 °C, 120 min	100	48	133
glucose	Fe−Sn-Beta	210 °C, 120 min	52	34	134
glucose	hierarchical Sn-Beta	160 °C, 0.5 MPa, 360 min	N/A	52 ML	13
glucose	hierarchical Zn−Sn-Beta	220 °C, 2 MPa, 360 min	100	67	135
glucose	hierarchical Fe−Sn-Beta	220 °C, 2 MPa, 360 min	100	67	136
cellulose	Er-Beta	240 °C, 2 MPa, 30 min	100	58	124
glucose	Er-ZSM-5	200 °C, 2 MPa, 30 min	100	72	8

calcination, probably due to the transition of open sites to closed sites, more prompt to assist retro-aldol, during calcination.[114] Addition of WO_3 particles in the reactor reduces the number of silanol groups, as WO_3 species adsorb on the silanol groups, which decreases the activation energy for glucose isomerization from 131 kJ mol^{-1} without WO_3 groups to 91 kJ mol^{-1} with the adsorption of the WO_3 groups, but it increases the general LA yields (Table 5). Glucose conversion decreases with the adsorption of WO_3, as less active silanol groups are available.[120]

Active site hydration happens for extraframework Sn_xO_y species in Sn−zeolitic systems.[122] SnO_2 is not a very active catalyst. Tin oxides also agglomerate and clutter the zeolite pores, which undermines the activity of the catalyst. The closed, intraframework species in hydrophobic pores typically have the highest activity for all the reaction steps except glucose isomerization.

The high reactivities of glucose and the intermediates to LA, combined with the high Lewis acidity of Sn zeolites, led to the conclusion that, for Sn-Beta catalyst at more than 120 °C, glucose diffusion in pores and adsorption strength are more determining than the intrinsic reaction rate.[123] As glucose is a relatively bulky molecule, pore size is a determining factor for isomerization to fructose. The 10-membered rings MFI[119] and ZSM-5 zeolites, having too small channels, do not show high activity for glucose reactions. Surprisingly, Er-ZSM-5 achieved 69% LA yield from glucose, for which Xiao et al. (2022) speculated that Er replaces the H in the −OH groups in the zeolitic framework, making it an accessible active group (Table 5).[8] On the other hand, inclusion of Er in the framework in the typical Si−O−M form was observed by Wang et al. (2017) with Beta zeolites, which have bigger channels than ZSM-5 zeolites, resulting in a 58% LA yield.[124] Topologies with larger rings, such as USY, MOR, MCM-41, SBA-15, BEA, and MWW do have channels large enough to enable good glucose diffusion.[99,125,126] Of all the zeolite topologies, the 12-membered BEA ring topology is the topology with the smallest channels able to act as a good host for glucose.

Although it takes a large pore size to get a guest−host interaction between the zeolite and glucose, microporosity assists the retro-aldol reaction by confining the steric interactions arising from the hydroxymethyl group on fructose's C1, stabilizing the TS and, thus, increasing the reaction rate.[137] Mesoporosity arising from desilication and dealumination lowers the LA yield from monosaccharides compared to smaller pore structures, as reaction intermediates are more likely to polymerize in large pores. Large pore systems offer higher LA yields from polysaccharides due to enhanced diffusion in the channels. The phenomenon was measured by Xia et al. (2021), achieving 33% LA yield from microalgae, with the main inhibition coming from lipids poisoning the active sites (Table 5).[136] The addition of formic acid induces controlled-release hydrolysis of microalgae, increasing the LA yield to 83% with a Sn-Beta catalyst (Table 5).[138] As for the Cannizzaro-type reaction from DHA to LA, small pore size does not seem to affect the catalytic performance, due to the small size of the C3 intermediates, in addition to the fact that DHA-to-PA dehydration is a thermal reaction and PA to LA is a fast reaction.[37,139] Moreover, large pore size leaves space for multiple small substrate molecules in a reactive environment, enhancing polymerization and humin formation, affecting the final LA yields.[127] The most suitable pore system to react glucose to LA is thus a combination of mesoporosity for glucose diffusion and microporosity to enhance fructose retro-aldol by confinement. This proposition is supported by the high yields achieved by hierarchical Sn-Beta zeolites possessing both a mesoporous and a microporous region (Table 5).[12−14,127] Bimetal hierarchical zeolites showed even better yields, with both Fe−Sn-Beta and Zn−Sn-Beta yielding 67% ML and displaying good reusability (Table 5).[134,135]

As with other catalysts, the catalyst/reactant ratio has to be high to maintain high reaction rates. For Sn-Beta as for other metal-functionalized zeolites, increasing the glucose concentration reduces the LA yield.[130] Indeed, glucose epimerization to mannose, fructose dehydration to 5-HMF catalyzed, and C3 polymerization to humins are slower reactions than the reaction steps leading to LA formation. For the same reasons, having too strong Lewis acid sites catalyzes faster glucose isomerization than retro-aldol, increasing fructose instantaneous concentration in the medium.[132] This fructose accumulation gives rise to more dehydration products such as 5-HMF and levulinic acid. To overcome fructose accumulation, Zhao et al. (2021) added γ-valerolactone to

Table 6. MOF Catalytic Performances for Sugar Reactions to LA

reactant	catalyst	conditions	conversion	LA yield	ref
xylose	Zr-UiO-66	170 °C, 240 min	98	78	151
glucose	Mg-MOF-74	200 °C, 180 min	100	27 ML	152
sucrose	ZIF-8	160 °C, 1440 min	N/A	42	153

Table 7. Photocatalyst Performances for Glucose Conversion to LA

reactant	catalyst	conditions	conversion	LA yield	ref
glucose	$Zn_{0.6}Cd_{0.4}S$, 1 M NaOH	360 min	90	78	17
xylose	CC_1@mCN, 2 M KOH	60 °C, 60 min	100	77	157
glucose	Ut-OCN, 3 M KOH	50 °C, 90 min	97	64	158
glucose	B@mCN-3, 2 M KOH	60 °C, 90 min	100	93	16

the water solvent, introducing competitive adsorption with glucose for the active sites, thus decreasing isomerization rates. This decreased instantaneous fructose concentration, which decreased the side reactions arising from a long fructose residence time (Table 5).[128] Sucrose is typically the sugar giving the highest LA yield, due to its slow degradation to glucose and fructose, keeping both their concentrations low and thus inhibiting side reactions, while being relatively easy to hydrolyze. Liu et al. (2022), using microwaves on the system, affected the isomerization equilibrium toward glucose, lowering glucose conversion, but at the same time increasing LA selectivity, due to low fructose concentration inhibiting side reactions (Table 5).[131] As Sn-Beta readily isomerizes glucose to fructose, but takes more time to proceed to retro-aldol due to its lack of strong acid sites, use of a bimetal catalyst helps to accelerate the reaction and hinder secondary reactions by avoiding fructose accumulation.[133,140,141] Xia et al. (2020) functionalized Beta zeolite with both Sn and In, achieving 53% LA yield from glucose, compared to 31% without the addition of indium.[132] In this system, indium decreased the Lewis acid site strength, slowing down the isomerization reaction from a kinetic constant of 0.0104 min^{-1} to 0.0061 min^{-1}, while it almost doubled the retro-aldol kinetic constant. It also had the effect of increasing mannose yields, but in a more modest way than it increased LA yields.[132]

One of the main reasons for the absence, to our knowledge, of large scale application of zeolites in biomass conversion is their fast deactivation. Different mechanisms explain this hardly avoidable fast deactivation. Rajabbeigi et al. (2014) stated that catalyst deactivation does not arise from byproduct presence but arises due to other factors.[142] The main deactivation mechanism is competitive solvent adsorption on active sites. Lewis acidity attracts water molecules, which promptly adsorb to framework and extraframework metal sites, making the active sites unavailable for the substrate.[143] Thus, a high metal content resulting in an increase of extraframework metals increases deactivation by hydration.[144] Although methanol adsorbs to a much smaller extent than water on the active sites, it tends to dehydrate open sites, reducing their catalytic activity. Adding less than 5% water in the methanol solvent improves the catalyst stability by keeping the active sites hydrated while avoiding water adsorption.[145] Brønsted acidity also causes C3 polymerization and other undesirable reactions, forming coke and humins adsorbing on the framework, deactivating the catalyst. Some surface groups, such as $-NH_3$, accelerate coke formation on the zeolite,[146] while water also enhances coke formation due to intrinsic Brønsted acidity at high temperature.[147] Placing the zeolite in

harsh hydrothermal conditions can also result in structural collapse, forming amorphous regions in the framework and extraframework metal agglomerates.[148] Although the collapse mechanism is not well described in the literature, it has been found that too harsh acid treatment causes amorphization. A Si/metal ratio smaller than 15 also increases the probability of structural collapse, and large pore size zeolites are more subject to structural change over the reaction runs.[126]

Metal leaching is also a cause for metal-functionalized zeolite deactivation, even though it is generally less important than the other causes mentioned above. Metal leaching happens more with postsynthesis functionalization than with hydrothermal synthesis, due to a weaker metal insertion in the framework.[107] As leaching is often more present with water versus methanol, Si−O−M bond hydrolysis might be a cause for this deactivation. Sn deactivates more in methanol due to higher Sn solubility in methanol than in water.[126] Metal leaching becomes a prominent problem when functionalizing the zeolitic framework with erbium as it has a very high affinity to water, which causes it to be more readily solubilized in the medium than to stay in the crystalline structure.[149,150]

Zeolites, and especially Sn-Beta zeolites, are effective catalysts to produce LA from biomass. Their long-term performances and reusability are influenced by the synthesis method and remain the main challenge to overcome to scale up a reactor using this catalyst. More efforts have to be made in using zeolites in continuous flow reactors to reach a higher technology readiness level.

Metal−Organic Frameworks (MOFs). Metal−organic frameworks (MOFs) as catalytic supports have recently drawn attention due to their high surface areas, well-defined pore systems, and capabilities for functionalization at their surfaces. Ponchai et al. (2020) grafted Zr on UiO-66, noting that Zr species were only at the surface of the framework, generating open sites.[151] Metal grafting dehydrates MOF surface oxygens, generating Lewis acid sites which readily catalyze glucose to LA.[154] Xylose reaction catalyzed by Zr-UiO-66 yields 78% LA after 4 h at 170 °C due to the presence of these Lewis acid sites (Table 6).[151] Guo et al. (2018) coupled Cr with MIL-101-GLY, leading to the same conclusion that the open sites at the surface of the MOFs brought Lewis acidity to the system, assisting the proton-transfer step in the glucose isomerization reaction. The active sites being on the surface, a higher surface/volume ratio increases catalytic activity.[155] Accordingly, Zn-ZIF-67 yielded more ML with smaller crystals, to reach a maximum at 42% ML from sucrose at 160 °C after 24 h (Table 6).[153] Mg-MOF-74 showed better activity than other MOFs with a higher

Table 8. Layered Double Hydroxide Performances for Glucose Conversion to LA

reactant	catalyst	conditions	conversion	LA yield	ref
glucose	MgAl LDH	150 °C, 600 min	N/A	38	15
glucose	CNT/LDH, 0.15 M NaOH, 2 M KOH	60 °C, 120 min	99	87	18

surface area.[152] Six-connectivity MOFs, such as MIL-101 and MOF-808, coordinate easier with their substrates than 8-connectivity MOFs like UiO-66. For 6-connectivity MOFs, the active oxygens at the surface of two different catalytic units coordinate with two carbons to promote the different reaction steps. Meanwhile, for 8-connectivity MOFs, only one catalytic unit coordinates with two carbons, thus forming a less stable reactive complex.[154,156] Hence, even though MOFs offer a stable guest−host interaction between the sugar and the catalyst, relatively low LA yields are achieved, leaving space for more studies on this type of support.

Photocatalysts. Almost all tested photocatalysts for the glucose reaction yielded over 75% LA (Table 7). Ma et al. (2020) transformed glucose with photocatalytic carbon nitride over different supports, finding that a graphitic structure doped with boron and oxygen achieved 80% LA yield, the highest reported by this research group.[16,157,158] A similar LA yield is achieved with a $Zn_{0.6}Cd_{0.4}S$ solid solution homojunction photocatalyst with a pseudoperiodic cubic zinc blende. This photocatalyst also coproduces H_2 during the glucose reaction, highlighting the possibility of a different reaction mechanism that is yet to be identified.[17] A CuO−chitosan hybrid hydrogel in a weak alkaline medium also displayed photocatalytic activity, reaching LA yields up to 82% from glucose.[159] The photocatalytic glucose reaction also operates at low temperature, as most studies identify 60 °C to be the optimal temperature (Table 7). Reusability is also found for these catalysts, highlighting a good potential for future commercialization. More extensive studies have to be carried to optimize the reaction, as only a very few studies have been published on the topic.

Layered Double Hydroxides. Layered double hydroxides (LDHs) are metallic oxygenated sheets held together by anions and water molecules forming a double layer of OH^-. These dual metal/base systems readily act as heterogeneous catalysts for glucose reactions, primarily due to their high Brønsted basicity. LDHs typically possess Mg and Al species as metals and CO_3^{2-} and NO_3^- as anions. Although Mg offers Brønsted base sites, it quickly loses activity due to the adsorption of intermediates on the active sites and fast leaching in water.[160−162] Water also adsorbs on hydrophilic sites, deactivating them.[163] These problems are less important in alcohol solvents, giving higher fructose yields at temperatures higher than 120 °C and ML yields at temperatures higher than 140 °C.[15] Ca/Al-hydrotalcites at 90 °C achieve a maximum 87% fructose selectivity from glucose. Strong basicity emerging from Ca complexes controls glucose conversion, while acidity arising from Al regulates fructose selectivity. At Ca/Al ratios greater than 3, EFCa is formed, giving $CaCO_3$. This causes Ca^{2+} cations to complex with the TS during the epimerization reaction, thus increasing mannose yields up to 65% due to high basicity and overall lack of acidity.[164] Ye et al. (2022) built a carbon nanotube/LDH composite catalyst, which develops photothermal activity in the matrix. Carbon nanotubes act as heating centers when exposed to light, increasing the internal temperature, while the LDHs provide Brønsted basicity and Lewis acidity, arising from oxygen vacancies.[18] With the

addition of 0.15 M NaOH, the LA yield went up to 86% from glucose, which is one of the highest yields observed to our knowledge (Table 8).

■ DISCUSSION

We have identified many of the most promising homogeneous and heterogeneous catalysts along with reaction mechanisms and challenges for scale-up and future research directions. Homogeneous catalysts are relatively simple to test, which accelerates testing and optimization versus heterogeneous systems. Thus, the highest LA yields observed to date from glucose have been produced with erbium salts as catalysts. However, the catalyst stability is poor and the environmental and safety considerations would increase capital and operating expenditures, which compromise any commercial interest. Nevertheless, Ma et al. (2023) performed a techno-economic analysis on a simulated plant producing 52 kt of LA/year working with $ErCl_3$ and calculated a payback period of 7.4 years based on a pessimistic LA selling price of 1250 USD/t.[55] Hence, even though the development stage of such a process is very low, an interest in pushing the research on the high-performance erbium homogeneous catalyst regarding its larger scale is potentially interesting.

The highest LA yields for heterogeneous catalysts have yet to match the maximum LA yields of homogeneous erbium catalysts. However, bifunctional zeolites are promising candidates, as they are relatively easy to synthesize, result in reasonable yields, and are more stable. As most of the deactivation comes from solvent adsorption and coking, coupling a regeneration unit to the catalytic reactor might overcome this challenge. Hence, more work on reactor design, catalyst regeneration, and techno-economic is warranted.

■ CONCLUSION

The characteristics of a catalyst able to achieve high LA yields from glucose and other related compounds have been identified, as well as the catalysts possessing these characteristics. For homogeneous catalysts, erbium salts achieve almost quantitative yields from glucose and cellulose due to their high Lewis acidities. However, erbium salts are expensive and suffer from low recyclability. Heterogeneous erbium catalysts suffer from metal leaching due to their high affinity with water, making them impossible to use at a larger scale. Moreover, the anion effect on salt catalysts is still a subject of discussion needing more experimental work. Yields over carbon supports and MOFs are, as of yet, too low for commercial application. The intrinsic acidities of zeolites are sufficient to drive the reaction, and these heterogeneous systems are easy to functionalize with various metals to improve activity. Hierarchical Sn-Beta catalysts are highly active catalysts due to their mesoporous structures with pores large enough to allow glucose diffusion, enabling isomerization to fructose, but they also provide a confinement effect to accelerate the fructose retro-aldol to highly reactive C3 intermediates. Well-tuned bimetallic zeolites have sufficient Lewis acidities to catalyze the reaction steps from glucose to LA while avoiding slow side reactions, making them very promising catalysts.

Zeolite deactivation is a critical issue needing more work in the future. Photocatalysts and LDHs yield more than 80% LA from glucose but need more extensive work for scale-up. As most of the studies tested catalysts in batch reactors, efforts have to be made to transpose these results in continuous flow to consider an industrial application. Some catalysts achieve performances promising enough to consider scale-up, but active site stability and low technological maturity are still major issues to overcome.

The most promising catalysts for industrial transformation of glucose to lactic acid are bimetallic hierarchical Sn-Beta zeolites.

■ AUTHOR INFORMATION

Corresponding Author

Gregory S. Patience − *Chemical Engineering, Polytechnique Montréal, Montréal H3T 1J4, Canada;* ● orcid.org/0000-0001-6593-7986; Email: gregory-s.patience@polymtl.ca

Author

Thomas Saulnier-Bellemare − *Chemical Engineering, Polytechnique Montréal, Montréal H3T 1J4, Canada*

Complete contact information is available at:
https://pubs.acs.org/10.1021/acsomega.3c10015

Notes

The authors declare no competing financial interest.

■ ACKNOWLEDGMENTS

■ ACRONYMS

DFT	density functional theory
DHA	dihydroxyacetone
DOSY NMR	diffusion ordered spectroscopy nuclear magnetic resonance
EL	ethyl lactate
LA	lactic acid
LDH	layered double hydroxide
ML	methyl lactate
MOF	metal−organic framework
PA	pyruvaldehyde
PLA	polylactic acid
TS	transition state
XRD	X-ray diffraction

■ REFERENCES

(1) *Bioplastics Market Size, Share & Trends Analysis Report By Product (Biodegradable, Non-biodegradable), By Application (Packaging, Agriculture; Consumer Goods, By Region, And Segment Forecasts, 2022−2030*; GVR-4-68038-587-8; Grand View Research: 2022.

(2) Msuya, N.; Katima, J. H. Y.; Masanja, E.; Temu, A. K. Poly(lactic-acid) Production_From Monomer to Polymer: A review. *Sci-Fed Journal of Polymer Science* **2017**, *1*, 1000002.

(3) Manandhar, A.; Shah, A. Techno-Economic Analysis of Bio-Based Lactic Acid Production Utilizing Corn Grain as Feedstock. *Processes* **2020**, *8*, 199.

(4) Kishida, H.; Jin, F.; Yan, X.; Moriya, T.; Enomoto, H. Formation of lactic acid from glycolaldehyde by alkaline hydrothermal reaction. *Carbohydr. Res.* **2006**, *341*, 2619−2623.

(5) Cantero, D. A.; Álvarez, A.; Bermejo, M. D.; Cocero, M. J. Transformation of glucose into added value compounds in a hydrothermal reaction media. *Journal of Supercritical Fluids* **2015**, *98*, 204−210.

(6) Wang, F.-F.; Liu, C.-L.; Dong, W.-S. Highly efficient production of lactic acid from cellulose using lanthanide triflate catalysts. *Green Chem.* **2013**, *15*, 2091−2095.

(7) Lei, X.; Wang, F.-F.; Liu, C.-L.; Yang, R.-Z.; Dong, W.-S. One-pot catalytic conversion of carbohydrate biomass to lactic acid using an ErCl3 catalyst. *Applied Catalysis A: General* **2014**, *482*, 78−83.

(8) Xiao, Y.; Liao, S.; Xu, S.; Li, J.; Lu, Z.; Hu, C. Selective transformation of typical sugars to lactic acid catalyzed by dealuminated ZSM-5 supported erbium. *Renewable Energy* **2022**, *187*, 551−560.

(9) Wang, F.-F.; Wu, H.-Z.; Ren, H.-F.; Liu, C.-L.; Xu, C.-L.; Dong, W.-S. Er/Beta-zeolite-catalyzed one-pot conversion of cellulose to lactic acid. *Journal of Porous Materials* **2017**, *24*, 697−706.

(10) Kim, K. H.; Kim, C. S.; Wang, Y.; Yoo, C. G. Integrated Process for the Production of Lactic Acid from Lignocellulosic Biomass: From Biomass Fractionation and Characterization to Chemocatalytic Conversion with Lanthanum(III) Triflate. *Ind. Eng. Chem. Res.* **2020**, *59*, 10832−10839.

(11) Yang, X.; Wu, L.; Wang, Z.; Bian, J.; Lu, T.; Zhou, L.; Chen, C.; Xu, J. Conversion of dihydroxyacetone to methyl lactate catalyzed by highly active hierarchical Sn-USY at room temperature. *Catalysis Science & Technology* **2016**, *6*, 1757−1763.

(12) Yang, X.; Bian, J.; Huang, J.; Xin, W.; Lu, T.; Chen, C.; Su, Y.; Zhou, L.; Wang, F.; Xu, J. Fluoride-free and low concentration template synthesis of hierarchical Sn-Beta zeolites: efficient catalysts for conversion of glucose to alkyl lactate. *Green Chem.* **2017**, *19*, 692−701.

(13) Tang, B.; Li, S.; Song, W.-C.; Yang, E.-C.; Zhao, X.-J.; Guan, N.; Li, L. Fabrication of Hierarchical Sn-Beta Zeolite as Efficient Catalyst for Conversion of Cellulosic Sugar to Methyl Lactate. *ACS Sustainable Chem. Eng.* **2020**, *8*, 3796−3808.

(14) Zhang, J.; Wang, L.; Wang, G.; Chen, F.; Zhu, J.; Wang, C.; Bian, C.; Pan, S.; Xiao, F.-S. Hierarchical Sn-Beta Zeolite Catalyst for the Conversion of Sugars to Alkyl Lactates. *ACS Sustainable Chem. Eng.* **2017**, *5*, 3123−3131.

(15) Ye, X.; Shi, X.; Zhong, H.; Wang, T.; Duo, J.; Jin, B.; Jin, F. Photothermal strategy for the highly efficient conversion of glucose into lactic acid at low temperatures over a hybrid multifunctional multi-walled carbon nanotube/layered double hydroxide catalyst. *Green Chem.* **2022**, *24*, 813−822.

(16) Ma, J.; Li, Y.; Jin, D.; Ali, Z.; Jiao, G.; Zhang, J.; Wang, S.; Sun, R. Functional B@mCN-assisted photocatalytic oxidation of biomass-derived pentoses and hexoses to lactic acid. *Green Chem.* **2020**, *22*, 6384−6392.

(17) Zhao, H.; Li, C.-F.; Yong, X.; Kumar, P.; Palma, B.; Hu, Z.-Y.; Van Tendeloo, G.; Siahrostami, S.; Larter, S.; Zheng, D.; Wang, S.; Chen, Z.; Kibria, M. G.; Hu, J. Coproduction of hydrogen and lactic acid from glucose photocatalysis on band-engineered Zn1-xCdxS homojunction. *iScience* **2021**, *24*, No. 102109.

(18) Ye, X.; Shi, X.; Xu, H.; Feng, Y.; Jin, B.; Duan, P. Enhanced catalytic activity of layered double hydroxides via in-situ reconstruction for conversion of glucose/food waste to methyl lactate in biorefinery. *Sci. Total Environ.* **2022**, *829*, 154540.

(19) Bandura, A. V.; Lvov, S. N. The Ionization Constant of Water over Wide Ranges of Temperature and Density. *J. Phys. Chem. Ref. Data* **2006**, *35*, 15.

(20) Matsuoka, S.; Kawamoto, H.; Saka, S. Retro-aldol-type fragmentation of reducing sugars preferentially occurring in polyether at high temperature: Role of the ether oxygen as a base catalyst. *Journal of Analytical and Applied Pyrolysis* **2012**, *93*, 24−32.

(21) Schandel, C. B.; Høj, M.; Osmundsen, C. M.; Jensen, A. D.; Taarning, E. Thermal Cracking of Sugars for the Production of Glycolaldehyde and Other Small Oxygenates. *ChemSusChem* **2020**, *13*, 688−692.

(22) Sasaki, M.; Goto, K.; Tajima, K.; Adschiri, T.; Arai, K. Rapid and selective retro-aldol condensation of glucose to glycolaldehyde in supercritical water. *Green Chem.* **2002**, *4*, 285−287.

(23) Kostetskyy, P.; Coile, M. W.; Terrian, J. M.; Collins, J. W.; Martin, K. J.; Brazdil, J. F.; Broadbelt, L. J. Selective production of glycolaldehyde via hydrothermal pyrolysis of glucose: Experiments and microkinetic modeling. *Journal of Analytical and Applied Pyrolysis* **2020**, *149*, No. 104846.

(24) Mainil, R.; Paksung, N.; Matsumura, Y. Determination of retro-aldol reaction type for glyceraldehyde under hydrothermal conditions. *Journal of Supercritical Fluids* **2019**, *143*, 370−377.

(25) Hutchinson, C. P.; Lee, Y. J. Evaluation of Primary Reaction Pathways in Thin-Film Pyrolysis of Glucose Using [13]C Labeling and Real-Time Monitoring. *ACS Sustainable Chem. Eng.* **2017**, *5*, 8796−8803.

(26) Cantero, D. A.; Vaquerizo, L.; Martinez, C.; Bermejo, M. D.; Cocero, M. J. Selective transformation of fructose and high fructose content biomass into lactic acid in supercritical water. *Catal. Today* **2015**, *255*, 80−86.

(27) Aida, T. M.; Tajima, K.; Watanabe, M.; Saito, Y.; Kuroda, K.; Nonaka, T.; Hattori, H.; Smith, R. L.; Arai, K. Reactions of d-fructose in water at temperatures up to 400°C and pressures up to 100 MPa. *Journal of Supercritical Fluids* **2007**, *42*, 110−119.

(28) Aida, T. M.; Ikarashi, A.; Saito, Y.; Watanabe, M.; Smith, R. L.; Arai, K. Dehydration of lactic acid to acrylic acid in high temperature water at high pressures. *Journal of Supercritical Fluids* **2009**, *50*, 257−264.

(29) Shen, Z.; Jin, F.; Zhang, Y.; Wu, B.; Kishita, A.; Tohji, K.; Kishida, H. Effect of Alkaline Catalysts on Hydrothermal Conversion of Glycerin into Lactic Acid. *Ind. Eng. Chem. Res.* **2009**, *48*, 8920−8925.

(30) Ma, C.; Jin, F.; Cao, J.; Wu, B. Hydrothermal Conversion of Carbohydrates into Lactic Acid with Alkaline Catalysts. *2010 4th International Conference on Bioinformatics and Biomedical Engineering*; IEEE: 2010; pp 1−4. DOI: 10.1109/ICBBE.2010.5516468.

(31) Yan, X.; Jini, F.; Kishita, A.; Enomoto, H.; Tohji, K. Formation of Lactic Acid from Cellulosic Biomass by Alkaline Hydrothermal Reaction. *AIP Conf. Proc.* **2008**, *987*, 50.

(32) Sánchez, C.; Serrano, L.; Llano-Ponte, R.; Labidi, J. Bread residues conversion into lactic acid by alkaline hydrothermal treatments. *Chemical Engineering Journal* **2014**, *250*, 326−330.

(33) Okuyama, T.; Kimura, K.; Fueno, T. Salt Effects on the Intramolecular Cannizzaro Reaction of Phenylglyoxal. Specific Acceleration by Calcium Ion. *Bull. Chem. Soc. Jpn.* **1982**, *55*, 2285−2286.

(34) Esposito, D.; Antonietti, M. Chemical Conversion of Sugars to Lactic Acid by Alkaline Hydrothermal Processes. *ChemSusChem* **2013**, *6*, 989−992.

(35) Li, L.; Shen, F.; Smith, R. L.; Qi, X. Quantitative chemocatalytic production of lactic acid from glucose under anaerobic conditions at room temperature. *Green Chem.* **2017**, *19*, 76−81.

(36) Yan, L.; Qi, X. Degradation of Cellulose to Organic Acids in its Homogeneous Alkaline Aqueous Solution. *ACS Sustainable Chem. Eng.* **2014**, *2*, 897−901.

(37) Yang, Q.; Sherbahn, M.; Runge, T. Basic Amino Acids as Green Catalysts for Isomerization of Glucose to Fructose in Water. *ACS Sustainable Chem. Eng.* **2016**, *4*, 3526−3534.

(38) Lux, S.; Siebenhofer, M. Synthesis of lactic acid from dihydroxyacetone: use of alkaline-earth metal hydroxides. *Catalysis Science & Technology* **2013**, *3*, 1380−1385.

(39) Li, L.; Yan, L.; Shen, F.; Qiu, M.; Qi, X. Mechanocatalytic Production of Lactic Acid from Glucose by Ball Milling. *Catalysts* **2017**, *7*, 170.

(40) Sánchez, C.; Egüés, I.; García, A.; Llano-Ponte, R.; Labidi, J. Lactic acid production by alkaline hydrothermal treatment of corn cobs. *Chemical Engineering Journal* **2012**, *181−182*, 655−660.

(41) Wang, Z.; Mo, C.; Xu, S.; Chen, S.; Deng, T.; Zhu, W.; Wang, H. Ca(OH)2 induced a controlled-release catalytic system for the efficient conversion of high-concentration glucose to lactic acid. *Molecular Catalysis* **2021**, *502*, 111406.

(42) Yan, X.; Jin, F.; Tohji, K.; Moriya, T.; Enomoto, H. Production of lactic acid from glucose by alkaline hydrothermal reaction. *J. Mater. Sci.* **2007**, *42*, 9995−9999.

(43) Zhao, Y.; Liu, R.; Marcus Pedersen, C.; Zhang, Z.; Guo, Z.; Chang, H.; Wang, Y.; Qiao, Y. Catalytic conversion of D-glucose into lactic acid with Ba(OH)2 as a base catalyst:mechanistic insight by NMR techniques. *J. Mol. Liq.* **2022**, *357*, 119074.

(44) Jeon, W.; Ban, C.; Park, G.; Woo, H. C.; Kim, D. H. Hydrothermal conversion of macroalgae-derived alginate to lactic acid catalyzed by metal oxides. *Catalysis Science & Technology* **2016**, *6*, 1146−1156.

(45) Bicker, M.; Endres, S.; Ott, L.; Vogel, H. Catalytical conversion of carbohydrates in subcritical water: A new chemical process for lactic acid production. *J. Mol. Catal. A: Chem.* **2005**, *239*, 151−157.

(46) Rasrendra, C. B.; Makertihartha, I. G. B. N.; Adisasmito, S.; Heeres, H. J. Green Chemicals from d-glucose: Systematic Studies on Catalytic Effects of Inorganic Salts on the Chemo-Selectivity and Yield in Aqueous Solutions. *Top. Catal.* **2010**, *53*, 1241−1247.

(47) Deng, W.; Wang, P.; Wang, B.; Wang, Y.; Yan, L.; Li, Y.; Zhang, Q.; Cao, Z.; Wang, Y. Transformation of cellulose and related carbohydrates into lactic acid with bifunctional Al(III)−Sn(II) catalysts. *Green Chem.* **2018**, *20*, 735−744.

(48) Wang, X.; Liang, F.; Huang, C.; Li, Y.; Chen, B. Highly active tin(IV) phosphate phase transfer catalysts for the production of lactic acid from triose sugars. *Catalysis Science and Technology* **2015**, *5*, 4410−4421.

(49) Wang, Y.; Deng, W.; Wang, B.; Zhang, Q.; Wan, X.; Tang, Z.; Wang, Y.; Zhu, C.; Cao, Z.; Wang, G.; Wan, H. Chemical synthesis of lactic acid from cellulose catalysed by lead(II) ions in water. *Nat. Commun.* **2013**, *4*, 2141.

(50) Zhou, L.; Wu, L.; Li, H.; Yang, X.; Su, Y.; Lu, T.; Xu, J. A facile and efficient method to improve the selectivity of methyl lactate in the chemocatalytic conversion of glucose catalyzed by homogeneous Lewis acid. *J. Mol. Catal. A: Chem.* **2014**, *388−389*, 74−80.

(51) Xu, S.; Wu, Y.; Li, J.; He, T.; Xiao, Y.; Zhou, C.; Hu, C. Directing the Simultaneous Conversion of Hemicellulose and Cellulose in Raw Biomass to Lactic Acid. *ACS Sustainable Chem. Eng.* **2020**, *8*, 4244−4255.

(52) Zhong, X.; Qing, Q.; Ji, H.; Jiang, S.; Wang, L. One-pot Conversion of Cellulose to Lactic Acid Catalyzed by Metal Ion Gd(3+) and A Detailed Analysis on the Product Distribution. *World Scientific Research Journal* **2020**, *6*, 270−278.

(53) Xu, S.; Li, J.; Li, J.; Wu, Y.; Xiao, Y.; Hu, C. D-Excess-LaA Production Directly from Biomass by Trivalent Yttrium Species. *iScience* **2019**, *12*, 132−140.

(54) Nguyen, V. C.; Dandach, A.; Vu, T. T. H.; Fongarland, P.; Essayem, N. ZrW catalyzed cellulose conversion in hydrothermal conditions: Influence of the calcination temperature and insights on the nature of the active phase. *Molecular Catalysis* **2019**, *476*, No. 110518.

(55) Ma, H.; Tingelstad, P.; Chen, D. Lactic acid production by catalytic conversion of glucose: An experimental and techno-economic evaluation. *Catal. Today* **2023**, *408*, 2−8.

(56) Liu, D.; Kim, K. H.; Sun, J.; Simmons, B. A.; Singh, S. Cascade Production of Lactic Acid from Universal Types of Sugars Catalyzed by Lanthanum Triflate. *ChemSusChem* **2018**, *11*, 598−604.

(57) Zhao, B.; Yue, X.; Li, H.; Li, J.; Liu, C.-L.; Xu, C.; Dong, W.-S. Lanthanum-modified phosphomolybdic acid as an efficient catalyst for the conversion of fructose to lactic acid. *Reaction Kinetics, Mechanisms and Catalysis* **2018**, *125*, 55−69.

(58) Wu, J.; Kim, K. H.; Jeong, K.; Kim, D.; Kim, C. S.; Ha, J.-M.; Chandra, R. P.; Saddler, J. N. The production of lactic acid from chemi-thermomechanical pulps using a chemo-catalytic approach. *Bioresour. Technol.* **2021**, *324*, 124664.

(59) Marianou, A.; Michailof, C.; Pineda, A.; Iliopoulou, E.; Triantafyllidis, K.; Lappas, A. Effect of Lewis and BrOnsted acidity on glucose conversion to 5-HMF and lactic acid in aqueous and organic media. *Applied Catalysis A: General* **2018**, *555*, 75−87.

(60) Hayashi, Y.; Sasaki, Y. Tin-catalyzed conversion of trioses to alkyl lactates in alcohol solution. *Chem. Commun.* 2005, 2716−2718.

(61) Zhang, W.; Xu, S.; Xiao, Y.; Qin, D.; Li, J.; Hu, C. The insights into the catalytic performance of rare earth metal ions on lactic acid formation from biomass via microwave heating. *Chemical Engineering Journal* 2021, 421, 130014.

(62) Elliot, S. G.; Tolborg, S.; Madsen, R.; Taarning, E.; Meier, S. Effects of Alkali-Metal Ions and Counter Ions in Sn-Beta-Catalyzed Carbohydrate Conversion. *ChemSusChem* 2018, 11, 1198−1203.

(63) Marianou, A. A.; Michailof, C. M.; Ipsakis, D. K.; Karakoulia, S. A.; Kalogiannis, K. G.; Yiannoulakis, H.; Triantafyllidis, K. S.; Lappas, A. A. Isomerization of Glucose into Fructose over Natural and Synthetic MgO Catalysts. *ACS Sustainable Chem. Eng.* 2018, 6, 16459−16470.

(64) Marianou, A. A.; Michailof, C. M.; Pineda, A.; Iliopoulou, E. F.; Triantafyllidis, K. S.; Lappas, A. A. Glucose to Fructose Isomerization in Aqueous Media over Homogeneous and Heterogeneous Catalysts. *ChemCatChem.* 2016, 8, 1100−1110.

(65) Udomcharoensab, T.; Praserthdam, P. A Comparative Study of the Divalent Transition Metal Oxide Supported on Magnesium Oxide Catalyst for Lactic Acid Production from Glucose. *IOP Conference Series: Materials Science and Engineering* 2019, 559, 012016.

(66) Nakajima, K.; Noma, R.; Kitano, M.; Hara, M. Titania as an Early Transition Metal Oxide with a High Density of Lewis Acid Sites Workable in Water. *J. Phys. Chem. C* 2013, 117, 16028−16033.

(67) Wang, X.; Song, Y.; Huang, L.; Wang, H.; Huang, C.; Li, C. Tin modified Nb2O5 as an efficient solid acid catalyst for the catalytic conversion of triose sugars to lactic acid. *Catalysis Science and Technology* 2019, 9, 1669−1679.

(68) Yamaguchi, S.; Yabushita, M.; Kim, M.; Hirayama, J.; Motokura, K.; Fukuoka, A.; Nakajima, K. Catalytic Conversion of Biomass-Derived Carbohydrates to Methyl Lactate by Acid−Base Bifunctional Gamma-Al2O3. *ACS Sustainable Chem. Eng.* 2018, 6, 8113−8117.

(69) Xiao, Y.; Xu, S.; Zhang, W.; Li, J.; Hu, C. One-pot chemo-catalytic conversion of glucose to methyl lactate over In/-Al2O3 catalyst. *Catal. Today* 2021, 365, 249−256.

(70) Zhao, X.; Wen, T.; Zhang, J.; Ye, J.; Ma, Z.; Yuan, H.; Ye, X.; Wang, Y. Fe-Doped SnO 2 catalysts with both BA and LA sites: facile preparation and biomass carbohydrates conversion to methyl lactate MLA. *RSC Adv.* 2017, 7, 21678−21685.

(71) Xu, H.; Ye, X.; Shi, X.; Zhong, H.; He, D.; Jin, B.; Jin, F. ZnO as a simple and facile catalyst for acid-base coordination transformation of biomass-based monosaccharides into lactic acid. *Molecular Catalysis* 2022, 522, 112241.

(72) Wattanapaphawong, P.; Reubroycharoen, P.; Yamaguchi, A. Conversion of cellulose into lactic acid using zirconium oxide catalysts. *RSC Adv.* 2017, 7, 18561−18568.

(73) Yang, L.; Su, J.; Carl, S.; Lynam, J. G.; Yang, X.; Lin, H. Catalytic conversion of hemicellulosic biomass to lactic acid in pH neutral aqueous phase media. *Applied Catalysis B: Environmental* 2015, 162, 149−157.

(74) Mylin, A. M.; Levytska, S. I.; Sharanda, M. E.; Brei, V. V. Selective conversion of dihydroxyacetone−ethanol mixture into ethyl lactate over amphoteric ZrO2−TiO2 catalyst. *Catal. Commun.* 2014, 47, 36−39.

(75) dos Santos, T. V.; da Silva Avelino, D. O.; Meneghetti, M. R.; Meneghetti, S. M. P. Mixed oxides based on SnO2 impregnated with MoO3: A robust system to apply in fructose conversion. *Catal. Commun.* 2018, 114, 120−123.

(76) Paulino, P. N.; Reis, O. C.; Licea, Y. E.; Albuquerque, E. M.; Fraga, M. A. Valorisation of xylose to lactic acid on morphology-controlled ZnO catalysts. *Catalysis Science and Technology* 2018, 8, 4945−4956.

(77) Kosri, C.; Kiatphuengporn, S.; Butburee, T.; Youngjun, S.; Thongratkaew, S.; Faungnawakij, K.; Yimsukanan, C.; Chanlek, N.; Kidkhunthod, P.; Wittayakun, J.; Khemthong, P. Selective conversion of xylose to lactic acid over metal-based Lewis acid supported on Gamma-Al2O3 catalysts. *Catal. Today* 2021, 367, 205−212.

(78) Pighin, E.; Díez, V. K.; Di Cosimo, J. I. Kinetic study of the ethyl lactate synthesis from triose sugars on Sn/Al2O3 catalysts. *Catal. Today* 2017, 289, 29−37.

(79) Prudius, S. V.; Hes, N. L.; Brei, V. V. Conversion of D-Fructose into Ethyl Lactate Over a Supported SnO2−ZnO/Al2O3 Catalyst. *Colloids and Interfaces* 2019, 3, 16.

(80) Hata, D.; Aihara, T.; Miura, H.; Shishido, T. Lactic Acid Production from Glucose over Y2O3-based Catalysts under Base-free Conditions. *Journal of the Japan Petroleum Institute* 2021, 64, 280−292.

(81) Li, H.; Ren, H.-F.; Zhao, B.-W.; Liu, C.-L.; Yang, R.-Z.; Dong, W.-S. Production of lactic acid from cellulose catalyzed by alumina-supported Er2O3 catalysts. *Res. Chem. Intermed.* 2016, 42, 7199−7211.

(82) Wang, X.; Song, Y.; Huang, C.; Wang, B. Crystalline niobium phosphates with water-tolerant and adjustable Lewis acid sites for the production of lactic acid from triose sugars. *Sustainable Energy and Fuels* 2018, 2, 1530−1541.

(83) Wang, Y.; Jin, F.; Sasaki, M.; Wahyudiono; Wang, F.; Jing, Z.; Goto, M. Selective conversion of glucose into lactic acid and acetic acid with copper oxide under hydrothermal conditions. *AIChE J.* 2013, 59, 2096−2104.

(84) Adam, Y. S.; Xu, Z.; Fang-ming, J.; Yan, F. Production of lactic acid from glucose with CuO as a catalyst under hydrothermal conditions. *2011 International Conference on Electrical and Control Engineering, Sept 16−18, 2011*; IEEE: 2011; pp 4635−4637.

(85) Younas, R.; Zhang, S.; Zhang, L.; Luo, G.; Chen, K.; Cao, L.; Liu, Y.; Hao, S. Lactic acid production from rice straw in alkaline hydrothermal conditions in presence of NiO nanoplates. *Catal. Today* 2016, 274, 40−48.

(86) Choudhary, H.; Ebitani, K. A Convenient Surfactant-Mediated Hydrothermal Approach to Control Supported Copper Oxide Species for Catalytic Upgrading of Glucose to Lactic Acid. *ChemNanoMat* 2015, 1, 511−516.

(87) Choudhary, H.; Nishimura, S.; Ebitani, K. Synthesis of high-value organic acids from sugars promoted by hydrothermally loaded Cu oxide species on magnesia. *Applied Catalysis B: Environmental* 2015, 162, 1−10.

(88) Ostervold, L.; Perez Bakovic, S. I.; Hestekin, J.; Greenlee, L. F. Electrochemical biomass upgrading: degradation of glucose to lactic acid on a copper(II) electrode. *RSC Adv.* 2021, 11, 31208−31218.

(89) Yu, I. K. M.; Xiong, X.; Tsang, D. C. W.; Ng, Y. H.; Clark, J. H.; Fan, J.; Zhang, S.; Hu, C.; Ok, Y. S. Graphite oxide- and graphene oxide-supported catalysts for microwave-assisted glucose isomer-isation in water. *Green Chem.* 2019, 21, 4341−4353.

(90) Yu, I. K. M.; Xiong, X.; Tsang, D. C. W.; Wang, L.; Hunt, A. J.; Song, H.; Shang, J.; Ok, Y. S.; Poon, C. S. Aluminium-biochar composites as sustainable heterogeneous catalysts for glucose isomerisation in a biorefinery. *Green Chem.* 2019, 21, 1267−1281.

(91) Xiong, X.; Yu, I. K. M.; Tsang, D. C. W.; Chen, L.; Su, Z.; Hu, C.; Luo, G.; Zhang, S.; Ok, Y. S.; Clark, J. H. Study of glucose isomerisation to fructose over three heterogeneous carbon-based aluminium-impregnated catalysts. *Journal of Cleaner Production* 2020, 268, No. 122378.

(92) Hou, G.-H.; Yan, L.-F. Synthesis of Pb(OH)2/rGO Catalyst for Conversion of Sugar to Lactic Acid in Water. *Chinese Journal of Chemical Physics* 2015, 28, 533−538.

(93) Kupila, R.; Lappalainen, K.; Hu, T.; Romar, H.; Lassi, U. Lignin-based activated carbon-supported metal oxide catalysts in lactic acid production from glucose. *Applied Catalysis A: General* 2021, 612, 118011.

(94) Kupila, R.; Lappalainen, K.; Hu, T.; Heponiemi, A.; Bergna, D.; Lassi, U. Production of ethyl lactate by activated carbon-supported Sn and Zn oxide catalysts utilizing lignocellulosic side streams. *Applied Catalysis A: General* 2021, 624, No. 118327.

(95) Wu, J.; Shen, L.; Duan, S.; Chen, Z.; Zheng, Q.; Liu, Y.; Sun, Z.; Clark, J.; Xu, X.; Tu, T. Selective Catalytic Dehydrogenative Oxidation of Bio-poyols to Lactic Acid. *Angew. Chem., Int. Ed.* 2020, 59, 13871−13878.

(96) Jimenez, M. V.; Ojeda-Amador, A. I.; Puerta-Oteo, R.; Martinez-Sal, J.; Passarelli, V.; Pérez-Torrente, J. J. Selective Oxidation of Glycerol via Acceptorless Dehydrogenation Driven by Ir(I)-NHC Catalysts. *Molecules* 2022, 27, 7666.

(97) Wu, J.; Shen, L.; Chen, Z.; Zheng, Q.; Xu, X.; Tu, T. Iridium-Catalyzed Selective Cross-Coupling of Ethylene Glycol and Methanol to Lactic Acid. *Angew. Chem., Int. Ed.* 2020, 59, 10421–10425.

(98) Chen, S.; Xu, S.; Ge, C.; Hu, C. Mechanistic Investigations of the Synthesis of Lactic Acid from Glycerol Catalyzed by an Iridium–NHC Complex. *Processes* 2022, 10, 626.

(99) Pang, J.; Zheng, M.; Li, X.; Song, L.; Sun, R.; Sebastian, J.; Wang, A.; Wang, J.; Wang, X.; Zhang, T. Catalytic Conversion of Carbohydrates to Methyl Lactate Using Isolated Tin Sites in SBA-15. *ChemistrySelect* 2017, 2, 309–314.

(100) Li, P.; Liu, G.; Wu, H.; Liu, Y.; Jiang, J.-g.; Wu, P. Postsynthesis and Selective Oxidation Properties of Nanosized Sn-Beta Zeolite. *J. Phys. Chem. C* 2011, 115, 3663–3670.

(101) Li, L.; Stroobants, C.; Lin, K.; Jacobs, P. A.; Sels, B. F.; Pescarmona, P. P. Selective conversion of trioses to lactates over Lewis acid heterogeneous catalysts. *Green Chem.* 2011, 13, 1175–1181.

(102) Verma, D.; Insyani, R.; Suh, Y.-W.; Kim, S. M.; Kim, S. K.; Kim, J. Direct conversion of cellulose to high-yield methyl lactate over Ga-doped Zn/H-nanozeolite Y catalysts in supercritical methanol. *Green Chem.* 2017, 19, 1969–1982.

(103) Dapsens, P. Y.; Mondelli, C.; Pérez-Ramírez, J. Highly Selective Lewis Acid Sites in Desilicated MFI Zeolites for Dihydroxyacetone Isomerization to Lactic Acid. *ChemSusChem* 2013, 6, 831–839.

(104) Graça, I.; Bacariza, M. C.; Fernandes, A.; Chadwick, D. Desilicated NaY zeolites impregnated with magnesium as catalysts for glucose isomerisation into fructose. *Applied Catalysis B: Environmental* 2018, 224, 660–670.

(105) Yang, X.; Wang, L.; Lu, T.; Gao, B.; Su, Y.; Zhou, L. Seed-assisted hydrothermal synthesis of Sn-Beta for conversion of glucose to methyl lactate: Effects of the H2O amount in the gel and crystallization time. *Catalysis Science and Technology* 2020, 10, 8437–8444.

(106) Botti, L.; Navar, R.; Tolborg, S.; Martinez-Espin, J. S.; Padovan, D.; Taarning, E.; Hammond, C. Influence of Composition and Preparation Method on the Continuous Performance of Sn-Beta for Glucose-Fructose Isomerisation. *Top. Catal.* 2019, 62, 1178–1191.

(107) Sun, Y.; Shi, L.; Wang, H.; Miao, G.; Kong, L.; Li, S.; Sun, Y. Efficient production of lactic acid from sugars over Sn-Beta zeolite in water: catalytic performance and mechanistic insights. *Sustainable Energy & Fuels* 2019, 3, 1163–1171.

(108) Yang, X.; Liu, Y.; Li, X.; Ren, J.; Zhou, L.; Lu, T.; Su, Y. Synthesis of Sn-Containing Nanosized Beta Zeolite As Efficient Catalyst for Transformation of Glucose to Methyl Lactate. *ACS Sustainable Chem. Eng.* 2018, 6, 8256–8265.

(109) Harris, J. W.; Cordon, M. J.; Di Iorio, J. R.; Vega-Vila, J. C.; Ribeiro, F. H.; Gounder, R. Titration and quantification of open and closed Lewis acid sites in Sn-Beta zeolites that catalyze glucose isomerization. *J. Catal.* 2016, 335, 141–154.

(110) Vega-Vila, J. C.; Harris, J. W.; Gounder, R. Controlled insertion of tin atoms into zeolite framework vacancies and consequences for glucose isomerization catalysis. *J. Catal.* 2016, 344, 108–120.

(111) Rai, N.; Caratzoulas, S.; Vlachos, D. G. Role of Silanol Group in Sn-Beta Zeolite for Glucose Isomerization and Epimerization Reactions. *ACS Catal.* 2013, 3, 2294–2298.

(112) Li, Y.-P.; Head-Gordon, M.; Bell, A. T. Analysis of the Reaction Mechanism and Catalytic Activity of Metal-Substituted Beta Zeolite for the Isomerization of Glucose to Fructose. *ACS Catal.* 2014, 4, 1537–1545.

(113) Bermejo-Deval, R.; Orazov, M.; Gounder, R.; Hwang, S.-J.; Davis, M. E. Active Sites in Sn-Beta for Glucose Isomerization to Fructose and Epimerization to Mannose. *ACS Catal.* 2014, 4, 2288–2297.

(114) Yang, X.; Lv, B.; Lu, T.; Su, Y.; Zhou, L. Promotion effect of Mg on a post-synthesized Sn-Beta zeolite for the conversion of glucose to methyl lactate. *Catalysis Science & Technology* 2020, 10, 700–709.

(115) Román-Leshkov, Y.; Moliner, M.; Labinger, J. A.; Davis, M. E. Mechanism of Glucose Isomerization Using a Solid Lewis Acid Catalyst in Water. *Angew. Chem., Int. Ed.* 2010, 49, 8954–8957.

(116) Christianson, J. R.; Caratzoulas, S.; Vlachos, D. G. Computational Insight into the Effect of Sn-Beta Na Exchange and Solvent on Glucose Isomerization and Epimerization. *ACS Catal.* 2015, 5, 5256–5263.

(117) Aho, A.; Kumar, N.; Eränen, K.; Lassfolk, R.; Mäki-Arvela, P.; Salmi, T.; Peurla, M.; Angervo, I.; Hietala, J.; Murzin, D. Y. Improving the methyl lactate yield from glucose over Sn−Al-Beta zeolite by catalyst promoters. *Microporous Mesoporous Mater.* 2023, 351, No. 112483.

(118) Iglesias, J.; Moreno, J.; Morales, G.; Melero, J. A.; Juárez, P.; López-Granados, M.; Mariscal, R.; Martínez-Salazar, I. Sn−Al-USY for the valorization of glucose to methyl lactate: switching from hydrolytic to retro-aldol activity by alkaline ion exchange. *Green Chem.* 2019, 21, 5876–5885.

(119) Gounder, R.; Davis, M. E. Beyond shape selective catalysis with zeolites: Hydrophobic void spaces in zeolites enable catalysis in liquid water. *AIChE J.* 2013, 59, 3349–3358.

(120) Yang, X.; Zhang, Y.; Zhou, L.; Gao, B.; Lu, T.; Su, Y.; Xu, J. Production of lactic acid derivatives from sugars over post-synthesized Sn-Beta zeolite promoted by WO3. *Food Chem.* 2019, 289, 285–291.

(121) Josephson, T. R.; DeJaco, R. F.; Pahari, S.; Ren, L.; Guo, Q.; Tsapatsis, M.; Siepmann, J. I.; Vlachos, D. G.; Caratzoulas, S. Cooperative Catalysis by Surface Lewis Acid/Silanol for Selective Fructose Etherification on Sn-SPP Zeolite. *ACS Catal.* 2018, 8, 9056–9065.

(122) Hammond, C.; Padovan, D.; Al-Nayili, A.; Wells, P. P.; Gibson, E. K.; Dimitratos, N. Identification of Active and Spectator Sn Sites in Sn-Beta Following Solid-State Stannation, and Consequences for Lewis Acid Catalysis. *ChemCatChem.* 2015, 7, 3322–3331.

(123) Tosi, I.; Sacchetti, A.; Martinez-Espin, J. S.; Meier, S.; Riisager, A. Exploring the Synthesis of Mesoporous Stannosilicates as Catalysts for the Conversion of Mono- and Oligosaccharides into Methyl Lactate. *Top. Catal.* 2019, 62, 628–638.

(124) Wang, J.; Yao, G.; Jin, F. One-pot catalytic conversion of carbohydrates into alkyl lactates with Lewis acids in alcohols. *Molecular Catalysis* 2017, 435, 82–90.

(125) Murillo, B.; Sanchez, A.; Sebastian, V.; Casado-Coterillo, C.; de la Iglesia, O.; Lopez-Ram-de Viu, M. P.; Tellez, C.; Coronas, J. Conversion of glucose to lactic acid derivatives with mesoporous Sn-MCM-41 and microporous titanosilicates. *J. Chem. Technol. Biotechnol.* 2014, 89, 1344–1350.

(126) Lari, G. M.; Dapsens, P. Y.; Scholz, D.; Mitchell, S.; Mondelli, C.; Pérez-Ramírez, J. Deactivation mechanisms of tin-zeolites in biomass conversions. *Green Chem.* 2016, 18, 1249–1260.

(127) Yang, L.; Yang, X.; Tian, E.; Vattipalli, V.; Fan, W.; Lin, H. Mechanistic insights into the production of methyl lactate by catalytic conversion of carbohydrates on mesoporous Zr-SBA-15. *J. Catal.* 2016, 333, 207–216.

(128) Zhao, X.; Zhou, Z.; Luo, H.; Zhang, Y.; Liu, W.; Miao, G.; Zhu, L.; Kong, L.; Li, S.; Sun, Y. Valerolactone-introduced controlled-isomerization of glucose for lactic acid production over an Sn-Beta catalyst. *Green Chem.* 2021, 23, 2634–2639.

(129) Holm, M. S.; Saravanamurugan, S.; Taarning, E. Conversion of Sugars to Lactic Acid Derivatives Using Heterogeneous Zeotype Catalysts. *Science* 2010, 328, 602–605.

(130) Kohler, A.; Seames, W.; Foerster, I.; Kadrmas, C. Catalytic Formation of Lactic and Levulinic Acids from Biomass Derived Monosaccharides through Sn-Beta Formed by Impregnation. *Catalysts* 2020, 10 (16), 1219.

(131) Liu, W.; Zhou, Z.; Guo, Z.; Wei, Z.; Zhang, Y.; Zhao, X.; Miao, G.; Zhu, L.; Luo, H.; Sun, M.; Wang, Y.; Li, S.; Kong, L. Microwave-induced controlled-isomerization during glucose conversion into lactic acid over a Sn-beta catalyst. *Sustainable Energy and Fuels* **2022**, *6*, 1264−1268.

(132) Xia, M.; Dong, W.; Shen, Z.; Xiao, S.; Chen, W.; Gu, M.; Zhang, Y. Efficient production of lactic acid from biomass-derived carbohydrates under synergistic effects of indium and tin in In−Sn-Beta zeolites. *Sustainable Energy & Fuels* **2020**, *4*, 5327−5338.

(133) Dong, W.; Shen, Z.; Peng, B.; Gu, M.; Zhou, X.; Xiang, B.; Zhang, Y. Selective Chemical Conversion of Sugars in Aqueous Solutions without Alkali to Lactic Acid Over a Zn-Sn-Beta Lewis Acid-Base Catalyst. *Sci. Rep.* **2016**, *6*, 26713.

(134) Cai, Q.; Yue, X.; Dong, W.-S. Hierarchical FeSn/Beta catalyzes the conversion of glucose to methyl lactate. *Journal of Porous Materials* **2021**, *28*, 1315−1324.

(135) Yue, X.-Y.; Ren, H.-F.; Wu, C.; Xu, J.; Li, J.; Liu, C.-L.; Dong, W.-S. Highly efficient conversion of glucose to methyl lactate over hierarchical bimetal-doped Beta zeolite catalysts. *J. Chem. Technol. Biotechnol.* **2021**, *96*, 2238−2248.

(136) Xia, M.; Shen, Z.; Gu, M.; Chen, W.; Dong, W.; Zhang, Y. Efficient catalytic conversion of microalgae residue solid waste into lactic acid over a Fe-Sn-Beta catalyst. *Sci. Total Environ.* **2021**, *771*, 144891.

(137) Zhu, Y.; Chuah, G.; Jaenicke, S. Chemo- and regioselective Meerwein−Ponndorf−Verley and Oppenauer reactions catalyzed by Al-free Zr-zeolite beta. *J. Catal.* **2004**, *227*, 1−10.

(138) Zan, Y.; Sun, Y.; Kong, L.; Miao, G.; Bao, L.; Wang, H.; Li, S.; Sun, Y. Formic Acid-Induced Controlled-Release Hydrolysis of Microalgae (Scenedesmus) to Lactic Acid over Sn-Beta Catalyst. *ChemSusChem* **2018**, *11*, 2492−2496.

(139) Wang, J.; Masui, Y.; Onaka, M. Conversion of triose sugars with alcohols to alkyl lactates catalyzed by Brønsted acid tin ion-exchanged montmorillonite. *Applied Catalysis B: Environmental* **2011**, *107*, 135−139.

(140) Xia, M.; Dong, W.; Gu, M.; Chang, C.; Shen, Z.; Zhang, Y. Synergetic effects of bimetals in modified beta zeolite for lactic acid synthesis from biomass-derived carbohydrates. *RSC Adv.* **2018**, *8*, 8965−8975.

(141) Xia, M.; Shen, Z.; Xiao, S.; Peng, B.-y.; Gu, M.; Dong, W.; Zhang, Y. Synergistic effects and kinetic evidence of a transition metal-tin modified Beta zeolite on conversion of Miscanthus to lactic acid. *Applied Catalysis A: General* **2019**, *583*, No. 117126.

(142) Rajabbeigi, N.; Torres, A. I.; Lew, C. M.; Elyassi, B.; Ren, L.; Wang, Z.; Je Cho, H.; Fan, W.; Daoutidis, P.; Tsapatsis, M. On the kinetics of the isomerization of glucose to fructose using Sn-Beta. *Chem. Eng. Sci.* **2014**, *116*, 235−242.

(143) van der Graaff, W. N. P.; Tempelman, C. H. L.; Li, G.; Mezari, B.; Kosinov, N.; Pidko, E. A.; Hensen, E. J. M. Competitive Adsorption of Substrate and Solvent in Sn-Beta Zeolite During Sugar Isomerization. *ChemSusChem* **2016**, *9*, 3145−3149.

(144) Li, L.; Collard, X.; Bertrand, A.; Sels, B. F.; Pescarmona, P. P.; Aprile, C. Extra-small porous Sn-silicate nanoparticles as catalysts for the synthesis of lactates. *J. Catal.* **2014**, *314*, 56−65.

(145) Padovan, D.; Botti, L.; Hammond, C. Active Site Hydration Governs the Stability of Sn-Beta during Continuous Glucose Conversion. *ACS Catal.* **2018**, *8*, 7131−7140.

(146) Shen, Z.; Kong, L.; Zhang, W.; Gu, M.; Xia, M.; Zhou, X.; Zhang, Y. Surface amino-functionalization of Sn-Beta zeolite catalyst for lactic acid production from glucose. *RSC Adv.* **2019**, *9*, 18989−18995.

(147) Zhang, Y.; Luo, H.; Zhao, X.; Zhu, L.; Miao, G.; Wang, H.; Li, S.; Kong, L. Continuous conversion of glucose into methyl lactate over the Sn-beta zeolite: Catalytic performance and activity insight. *Ind. Eng. Chem. Res.* **2020**, *59*, 17365−17372.

(148) Zhang, Y.; Luo, H.; Kong, L.; Zhao, X.; Miao, G.; Zhu, L.; Li, S.; Sun, Y. Highly efficient production of lactic acid from xylose using Sn-beta catalysts. *Green Chem.* **2020**, *22*, 7333−7336.

(149) Wang, F.-F.; Liu, J.; Li, H.; Liu, C.-L.; Yang, R.-Z.; Dong, W.-S. Conversion of cellulose to lactic acid catalyzed by erbium-exchanged montmorillonite K10. *Green Chem.* **2015**, *17*, 2455−2463.

(150) Tallarico, S.; Costanzo, P.; Bonacci, S.; Macario, A.; Di Gioia, M. L.; Nardi, M.; Procopio, A.; Oliverio, M. Combined Ultrasound/ Microwave Chemocatalytic Method for Selective Conversion of Cellulose into Lactic Acid. *Sci. Rep.* **2019**, *9*, No. 18858.

(151) Ponchai, P.; Adpakpang, K.; Thongratkaew, S.; Chaipojjana, K.; Wannapaiboon, S.; Siwaipram, S.; Faungnawakij, K.; Bureekaew, S. Engineering zirconium-based UiO-66 for effective chemical conversion of D-xylose to lactic acid in aqueous condition. *Chem. Commun.* **2020**, *56*, 8019−8022.

(152) Lu, X.; Wang, L.; Lu, X. Catalytic conversion of sugars to methyl lactate over Mg-MOF-74 in near-critical methanol solutions. *Catal. Commun.* **2018**, *110*, 23−27.

(153) Murillo, B.; Zornoza, B.; De La Iglesia, O.; Tellez, C.; Coronas, J. Chemocatalysis of sugars to produce lactic acid derivatives on zeolitic imidazolate frameworks. *J. Catal.* **2016**, *334*, 60−67.

(154) Rojas-Buzo, S.; Corma, A.; Boronat, M.; Moliner, M. Unraveling the Reaction Mechanism and Active Sites of Metal− Organic Frameworks for Glucose Transformations in Water: Experimental and Theoretical Studies. *ACS Sustainable Chem. Eng.* **2020**, *8*, 16143−16155.

(155) Guo, Q.; Ren, L.; Kumar, P.; Cybulskis, V. J.; Mkhoyan, K. A.; Davis, M. E.; Tsapatsis, M. A Chromium Hydroxide/MIL-101(Cr) MOF Composite Catalyst and Its Use for the Selective Isomerization of Glucose to Fructose. *Angew. Chem.* **2018**, *130*, 5020−5024.

(156) Luo, Q.-X.; Zhang, Y.-B.; Qi, L.; Scott, S. L. Glucose Isomerization and Epimerization over Metal-Organic Frameworks with Single-Site Active Centers. *ChemCatChem.* **2019**, *11*, 1903− 1909.

(157) Ma, J.; Jin, D.; Li, Y.; Xiao, D.; Jiao, G.; Liu, Q.; Guo, Y.; Xiao, L.; Chen, X.; Li, X.; Zhou, J.; Sun, R. Photocatalytic conversion of biomass-based monosaccharides to lactic acid by ultrathin porous oxygen doped carbon nitride. *Applied Catalysis B: Environmental* **2021**, *283*, 119520.

(158) Ma, J.; Li, Y.; Jin, D.; Yang, X.; Jiao, G.; Liu, K.; Sun, S.; Zhou, J.; Sun, R. Reasonable regulation of carbon/nitride ratio in carbon nitride for efficient photocatalytic reforming of biomass-derived feedstocks to lactic acid. *Applied Catalysis B: Environmental* **2021**, *299*, No. 120698.

(159) Li, Y.; Ma, J.; Jin, D.; Jiao, G.; Yang, X.; Liu, K.; Zhou, J.; Sun, R. Copper oxide functionalized chitosan hybrid hydrogels for highly efficient photocatalytic-reforming of biomass-based monosaccharides to lactic acid. *Applied Catalysis B: Environmental* **2021**, *291*, No. 120123.

(160) Delidovich, I.; Palkovits, R. Catalytic activity and stability of hydrophobic Mg−Al hydrotalcites in the continuous aqueous-phase isomerization of glucose into fructose. *Catalysis Science & Technology* **2014**, *4*, 4322−4329.

(161) Delidovich, I.; Palkovits, R. Structure−performance correlations of Mg−Al hydrotalcite catalysts for the isomerization of glucose into fructose. *J. Catal.* **2015**, *327*, 1−9.

(162) Yabushita, M.; Shibayama, N.; Nakajima, K.; Fukuoka, A. Selective Glucose-to-Fructose Isomerization in Ethanol Catalyzed by Hydrotalcites. *ACS Catal.* **2019**, *9*, 2101−2109.

(163) Yu, I. K. M.; Hanif, A.; Tsang, D. C. W.; Shang, J.; Su, Z.; Song, H.; Ok, Y. S.; Poon, C. S. Tuneable functionalities in layered double hydroxide catalysts for thermochemical conversion of biomass-derived glucose to fructose. *Chemical Engineering Journal* **2020**, *383*, No. 122914.

(164) Ventura, M.; Cecilia, J. A.; Rodríguez-Castellón, E.; Domine, M. E. Tuning Ca−Al-based catalysts' composition to isomerize or epimerize glucose and other sugars. *Green Chem.* **2020**, *22*, 1393− 1405.